



Chronometric data and stratigraphic evidence support discontinuity between Neanderthals and early *Homo sapiens* in the Italian Peninsula

Received: 11 December 2023

Accepted: 9 August 2024

Published online: 13 September 2024

Check for updates

Tom Higham 1,2, 12, Marine Frouin 3,12 , Katerina Douka 1,2, Annamaria Ronchitelli⁴, Paolo Boscato⁴, Stefano Benazzi⁵, Jacopo Crezzini^{4,6}, Vincenzo Spagnolo 4,7, Maxine McCarty 8, Giulia Marciani^{4,5}, Armando Falcucci 9, Matteo Rossini⁴, Simona Arrighi^{4,5,7}, Clarissa Dominici 4, Thibaut Devière 10, Jean-Luc Schwenninger¹¹, Ivan Martini⁴, Adriana Moroni^{4,7,12} & Francesco Boschin 4,12

The process by which Palaeolithic Europe was transformed from a Neanderthal-dominated region to one occupied exclusively by *Homo sapiens* has proven challenging to diagnose. A blurred chronology has made it difficult to determine when Neanderthals disappeared and whether modern humans overlapped with them. Italy is a crucial region because here we can identify not only Late Mousterian industries, assumed to be associated with Neanderthals, but also early Upper Palaeolithic industries linked with the appearance of early *H. sapiens*, such as the Uluzzian and the Aurignacian. Here, we present a chronometric dataset of 105 new determinations (74 radiocarbon and 31 luminescence ages) from four key southern Italian sites: Cavallo, Castelcivita, Cala, and Oscurusciuto. We built Bayesian-based chronometric models incorporating these results alongside the relative stratigraphic sequences at each site. The results suggest: 1) that the disappearance of Neanderthals probably pre-dated the appearance of early modern humans in the region and; 2) that there was a partial overlap in the chronology of the Uluzzian and Protoaurignacian, suggesting that these industries may have been produced by different human groups in Europe.

Between 50 and 35 thousand years ago, local Western Eurasian populations were progressively replaced by modern humans (*Homo sapiens*) originally stemming from the African continent. Europe at this time was characterised by a kaleidoscope of cultural entities, which exhibited a variety of stone tool production modes, ornamental practices, and hunting strategies, reflecting diverse techno-cultural approaches to interacting with the environment. There are four main groups: the Mousterian technocomplexes, generally attributed to

Neanderthals: the so-called “transitional industries”, for several decades all attributed to the last Neanderthals¹ (Châtelperronian in France, Uluzzian in Italy and Greece, Szeletian in Czech Republic and Hungary, and Lincombian-Ranisian-Jerzmanowician (LRJ) in southern UK, Belgium, Germany and Poland); the Initial Upper Palaeolithic (IUP—in Bulgaria and Moravia), recently linked with modern humans; and, from ~4 to 40 ka cal BP, the Aurignacian technocomplexes (Protoaurignacian and Early Aurignacian), considered a reliable proxy for the

A full list of affiliations appears at the end of the paper. e-mail: thomas.higham@univie.ac.at; marine.frouin@stonybrook.edu; francesco.boschin@unisi.it

presence of *H. sapiens*^{2–4}. Most of these technocomplexes exist in the Italian Peninsula, hence the region plays a crucial role, with numerous archaeological sites with key stratigraphic sequences documenting the period.

Over the last decade, many dates have been obtained from Italian sites that solidify the general temporal picture of the region. Previous determinations were dominated by results that significantly underestimated their real age^{5,6}. Despite this progress, several questions remain open which could be answered with improved chronometric modelling. One of the most pressing is the issue of the chronological spread of the Uluzzian in relation to preceding Mousterian occupations and the possibility of regional variations in its earlier occurrence. Did the Uluzzian groups colonise territories already empty, or did they come in direct contact with previous inhabitants? Is it possible that their appearance was broadly contemporaneous across the greater region in which it has been identified? Given that the start of the Uluzzian can be seen as the end of Mousterian populations at a specific site, it becomes crucial to document the start and chronological extent of this technocomplex at a regional scale. Another intriguing question is concerned with the apparently rapid disappearance of the Uluzzian in the archaeological record and its relationships with the emergence of the Aurignacian: are we dealing with a mere replacement of one group by another, as suggested by the stratigraphic evidence at certain sites? Or, are we seeing a rapid integration between the previous occupants and the newcomers, as it seems to be hinted at in the lithic industries of the last Uluzzian groups in sites such as Grotta del Cavallo and Grotta della Cala? Exploring the question of the Aurignacian, and especially its earliest phase, the Protoaurignacian, may provide insights into clarifying this issue.

In this paper, we present 105 radiocarbon and luminescence age determinations obtained from four key archaeological sequences in southern Italy that have the potential to resolve these questions. The sites include Grotta del Cavallo, Grotta di Castelcivita, Grotta della Cala and Riparo l'Oscurusciuto. We aim to (1) obtain a reliable regional framework of the final presence of the Mousterian, of the arrival/demise of the Uluzzian and of the arrival of the Aurignacian in southern Italy; (2) test whether the integration of chronological and stratigraphic data could suggest or exclude possible interactions between Mousterian/Uluzzian and Uluzzian/Aurignacian in central-southern Italy; and (3) make inferences at a supra-regional scale regarding the dispersal times and routes of *H. sapiens* throughout the peninsula, making direct comparisons between northern and southern Italy.

Recent work has significantly improved our understanding of the variability present in archaeological technocomplexes in Italy and this has helped considerably in understanding the processes underlying the Middle to Upper Palaeolithic transition. The final stage of the Mousterian in the Italian Peninsula is primarily characterised by Levallois and discoid production methods, which involve careful preparation of the core to obtain flakes, elongated blanks, blades, and, occasionally, bladelets. The shift towards more laminar and even lamellar production is a trend mirrored across Europe^{7,8}. During the Mousterian, local raw material sources were favoured⁷ and symbolic behaviour was generally absent (Fig. 1). The early phases of the Aurignacian in Italy are characterised by both the so-called Proto and Early cultural variants, found consistently in chronostratigraphic succession. Both variants exhibit systematic bladelet production. In the Protoaurignacian, bladelets were derived from the reduction of platform cores, while in the Early Aurignacian a notable increase in the utilisation of carinated cores, likely associated with increased mobility among hunter-gatherers⁹, is observed. Bladelets were probably employed as inserts in mechanically delivered projectiles¹⁰ and, in the Protoaurignacian, they were frequently modified through marginal retouching¹¹. Polished bone tools, personal ornaments and the use of colouring substances are extensively documented during the Italian

Aurignacian¹² (Fig. 1) along with several objects of portable art (e.g., ref. 13).

Prior to 2011, the Uluzzian was a transitional group of assemblages found at several sites, and linked with Neanderthals, mostly due to an alleged similarity with the Châtelperronian. The reanalysis in 2011 of two deciduous human teeth recovered in 1964 at Grotta del Cavallo (southern Italy), the site in which the Uluzzian was initially described¹⁴, suggested that the teeth belonged to modern humans¹⁵, dating at ~45–43 ka cal BP (thousand years before present). This, in turn, meant that *H. sapiens* were present in Europe at least as early as this (at the time, the Grotta del Cavallo dates were the earliest dates associated with modern humans in Europe). Since then, the presence of even earlier occurrences of *H. sapiens* at Bacho Kiro¹⁶ and Grotte Mandrin¹⁷, in association with IUP industries, has shown that *H. sapiens* were present in Europe even before the Uluzzian.

Recent work has shown the closer behavioural affinity of the Uluzzian with the Upper Palaeolithic than with Mousterian human groups (Fig. 1) due to important differences in subsistence strategies, including the use of mechanically delivered weapons (use of bow and/or spear thrower), the significant role played by personal ornaments and colouring substances, as well as the systematic production of polished bone tools. In addition, a distinctive feature of the Uluzzian lies in the fact that it consists of a flake-bladelet-based industry with a predominant use of bipolar knapping on anvil, a production system conceptually very different from those in use in the Mousterian^{7,18–26}.

The re-evaluation of the Uluzzian, besides overturning the previous attribution of the technocomplex to Neanderthals (although see ref. 27 for an alternative view), raised doubts regarding the attribution of the remaining “transitional” assemblages to Neanderthals. Mylopotamitaki et al.²⁸ demonstrated recently that the LRJ technocomplex at the site of Ranis-Ilsenhöhle was probably produced by *H. sapiens* too, confirming the suspicions of other researchers²⁹. Finally, some scholars have posited that the Châtelperronian technocomplex could also be linked with *H. sapiens*, as its industry displays Upper Palaeolithic-like techno-typological characteristics rather than reflecting previous Mousterian traditions^{30,31}. Hence, the concept of “transitional industries”, conventionally positioned at the middle to upper Palaeolithic boundary, and indeed the very term “transitional”, are becoming increasingly questioned and progressively losing their relevance and meaning due to the absence of any direct filiation from the preceding Mousterian industries.

Stratigraphically, the Uluzzian is always found above the Mousterian, and a sedimentological unconformity is present in most cases between the two⁷. In Italy, sites are located in the north-eastern (Grotta di Fumane and Riparo Broion³²), in the central (Grotta La Fabbrica, Tuscany, and Colle Rotondo, Latium^{33,34}) and especially in the southern part of the peninsula, where the most important stratigraphic sequences occur (e.g., Grotta del Cavallo, Grotta Riparo di Uluzzo C, Grotta di Serra Cicora, Grotta Mario Bernardini, Grotta della Cala, Grotta di Castelcivita and Grotta Roccia San Sebastiano²⁴). In central-southern Italy, the earliest phases of the Aurignacian were identified in some of the above-mentioned Uluzzian sites (Grotta la Fabbrica, Grotta di Serra Cicora, Grotta della Cala and Grotta di Castelcivita) where they consistently overlie the Uluzzian occupation very often with a stratigraphic discontinuity (e.g., sterile sediments, sedimentological hiatus, erosional event) in between (Fig. 2). In certain northern Italian sites, such as Riparo Mochi and Riparo Bombrini, where the Uluzzian is absent, a stratigraphic hiatus is also observed. This hiatus is marked by an erosive event, creating a clear division between the Late Mousterian and the subsequent Protoaurignacian layers^{3,7}. The four sites we investigate in this work are all found in the central-southern regions of Italy.

Grotta del Cavallo, hereafter referred to as Cavallo, contains a deep 7 m-thick archaeological sequence that encompasses the Middle

Palaeolithic (layers N-F), the Uluzzian (layers E-D), the final Upper Palaeolithic (layer B Romanellian), and the Neolithic (layer A)³⁵. The Uluzzian sequence, divided into three main cultural phases (layer EII archaic, layers EII-I evolved, and layer D final), sits between two tephra layers, termed Fa (below) and CII (above) (Supplementary Fig. 1). Layer

Fa has been attributed to the Y-6 tephra (Green Tuff of Pantelleria Island) dated to 45.5 ± 1.0 ka³⁶, while CII has been identified as the Y-5 eruption (Campanian Ignimbrite) dated to 39.85 ± 0.14 ka³⁷. The association between Late Mousterian/Neanderthals has been confirmed by the occurrence of Neanderthal human remains in layer EII³⁸.



Fig. 1 | Schematic example of the cultural evidence characterising the Late Mousterian, the Uluzzian and the Aurignacian in southern Italy. Mousterian: Levallois core (1); Levallois points (2–3 and 6–9) and side-scrapers (4–5) from Ossuruscrito. Uluzzian: bipolar core (10), bipolar blade (11), refitting (12) and lunates from Cavallo (13–14) and Castelcivita (15); bone tools from Cavallo (16–17), Castelcivita (18–19) and Cala (20); *Antalis vulgaris* (21), *Homalopoma sanguineum* (22) and *Glycimeris nummaria* (23) from Castelcivita; *Columbella rustica* (24), *Tritia neritea* (25) and *Antalis* sp. (26) from Cavallo. Aurignacian: prismatic core (27) and bladelet production (28) from the Protoaurignacian of Castelcivita; Bone tools (29–30) from the Aurignacian of La Cala; *Homalopoma sanguineum* (31), *Tritia*

incrassata (32), *Trivia mediterranea* (33), *Tritia mutabilis* (34), *Gibbula ardens* (35) from the Aurignacian of La Cala and a fragment of *Pecten jacobaeus* (36) from the Protoaurignacian of Castelcivita; prismatic core (carinated end scraper) (37) and bladelet production (38) from the Early Aurignacian of Castelcivita; Bone tool (39) from the Early Aurignacian of Castelcivita; *Homalopoma sanguineum* (40), *Clanculus corallinus* (41), *Glycimeris nummaria* (42), *Tritia mutabilis* (43) and *Columbella rustica* (44) from the Early Aurignacian of Castelcivita. The lithic and bone tools are scaled to each other, while the ornaments are on a different scale. The taxonomic attribution of shells is from Tassoni and see Ref. 98.

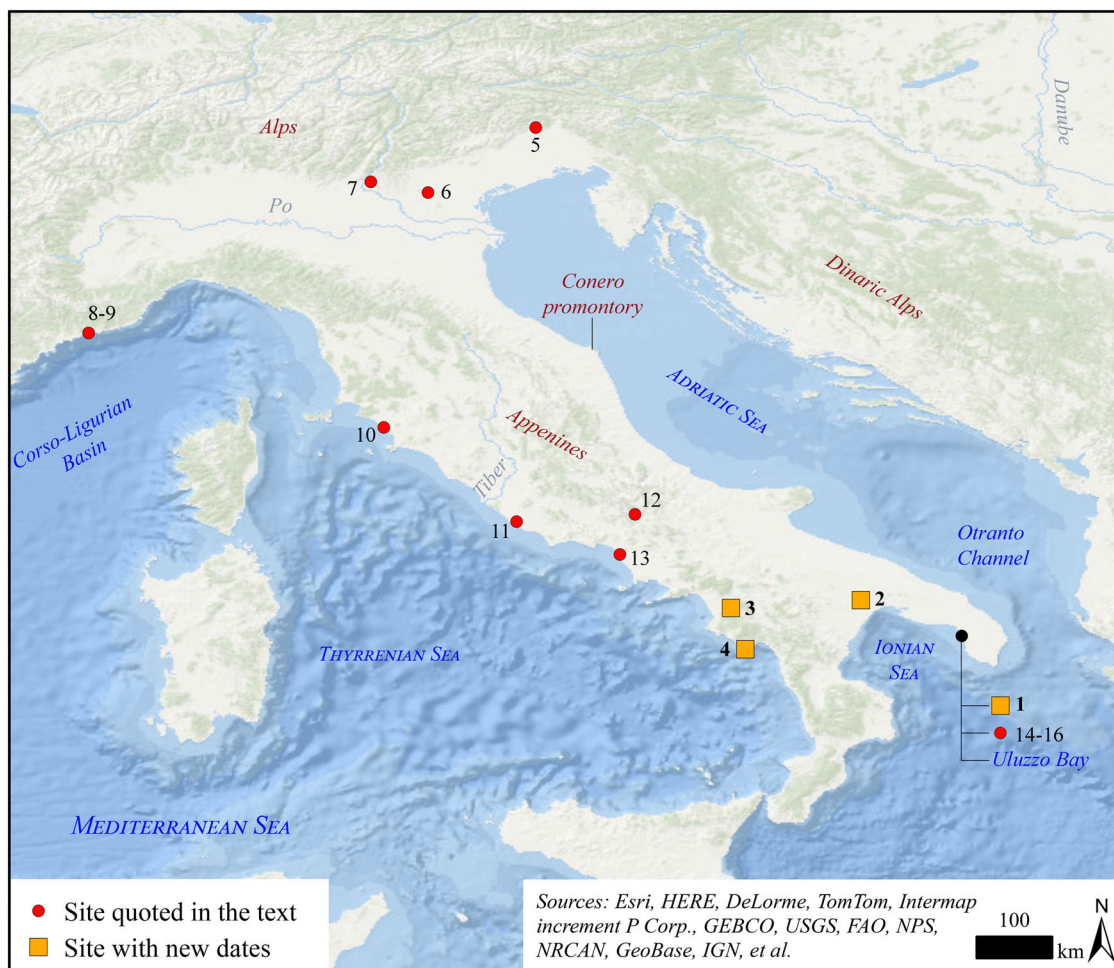


Fig. 2 | Map of the Italian Peninsula showing the location of the Italian sites considered in this paper. 1) Grotta del Cavallo; 2) Riparo L'Oscurusciuto; 3) Grotta di Castelcivita; 4) Grotta della Cala; 5) Grotta di Rio Secco; 6) Riparo del Broion; 7) Grotta di Fumane; 8) Riparo Bombrini; 9) Riparo Mochi; 10) Grotta della Fabbrica;

11) Colle Rotondo; 12) Grotta Reali; 13) Roccia San Sebastiano; 14) Grotta di Serra Cicora; 15) Grotta di Uluzzo C; 16) Grotta Mario Bernardini. Sources of the basemap: Esri, HERE, DeLorme, TomTom, Intermap increment P Corp., GEBCO, USGS, FAO, NPS, NRCAN, GeoBase, IGN, et al. The map was generated using ArcGIS®10.8.

Grotta di Castelcivita, hereafter referred to as Castelcivita, is in the Cilento region and covers the entirety of the Middle to Upper Palaeolithic transition (Late Mousterian, Uluzzian, Protoaurignacian and Early Aurignacian). The lowermost Mousterian layer (cgr) was previously radiocarbon dated at $39,000 \pm 1300$ and $42,700 \pm 900$ BP, but it was accepted that these ages were likely to be significant underestimates. A date of $36,120 \pm 360$ BP was obtained for the uppermost Uluzzian layer rsa^{39,40}. The anthropogenic sequence is sealed at its top by a multilayered flowstone in which volcanic layers attributable to the Y-5 (Campanian Ignimbrite) eruption lie interbedded. A sedimentological unconformity is present between the last Mousterian and the initial Uluzzian occupation (Supplementary Fig. 2).

Grotta della Cala, hereafter referred to as Cala, is a coastal site also in the Cilento region. Two main areas were excavated: the first a trench of ~12 m² and ~3 m-deep, located in the middle of the cave and named “internal series”. The second, 28 m² in size, is close to the cave entrance and is known as the “atrium series”. The whole archaeological succession of Cala covers a period of ca. 70 ka, from the Mousterian to the Bronze age, including a critical and detailed Upper Palaeolithic series starting with the Uluzzian and the Aurignacian⁴¹. A change in sedimentation is visible between the Mousterian and the Uluzzian, and the Uluzzian and Aurignacian (Supplementary Fig. 3). In the atrium, previous dates from the Cala

Aurignacian, Uluzzian and Mousterian layers have been surprisingly at odds with the pattern established at other sites, with radiocarbon dates much more recent than expected. A part was obtained in the 1970s by the Florence Radiocarbon Laboratory⁴² and others in the 1990s by the Oxford Radiocarbon Accelerator Unit (ORAU)⁴³. All determinations were obtained on charcoal or burnt bone and were substantially too young for their contexts. We attribute this to the ill-advised selection of burnt bone, which is known to often underestimate the real age, and to the lack of robust pretreatment for the charcoal samples. We consider these results best left out of discussion of the site chronology.

Riparo l'Oscurusciuto, also named Oscurusciuto, is a sheltered site located in the ravine of Ginosa at about 20 km from the present-day Ionian coastline. The site preserves a deposit about 6 m-thick located at the bottom of a steep rock wall, containing evidence for several Mousterian layers^{44–46}. In the excavated part, a Mousterian living floor (stratigraphic unit 15) sealed by a volcanic eruption dated at 55 ± 2 ka (Mount Epomeo Green Tuff–stratigraphic unit 14^{47,48}) has been revealed (Supplementary Fig. 4). The overlying stratigraphic units have yielded an almost continuous Mousterian occupation ending at ~40–42 ka cal. BP (at 95.4% probability), according to the only radiocarbon date available at the base of stratigraphic unit 1⁴⁹. In the uppermost stratigraphic units (4–1), the excavated area is highly reduced due to erosive processes.

Table 1 | Radiocarbon analytical data AMS dates for the site of Castelcivita

OxA	Material	Layer/spit/square	Industry	Species/ZooMS id	Pcode	^{14}C age BP	\pm error	fM	\pm error	$\delta^{13}\text{C}$ (‰)
X-2698-45	charcoal	GIC Focolare L11/12	Early Aurignacian	Not identified	YR	34,380	310	0.01385	0.00054	-24.8
22622	charcoal	RSA", 11	Uluzzian	c.f. <i>Ilex aquifolium</i>	XR	36,120	360	0.01114	0.0005	-24.8
X-2770-41	bone	RSA" lower 11 F14 II	Uluzzian	Cervid	AF	38,300	1000	0.00848	0.00104	-19.3
X-2770-40	bone	RSA" lower 11 F14 II	Uluzzian	Equid	AF	38,300	1000	0.00855	0.00104	-20.1
X-2770-39	bone	RSA" lower 11 F14 IV	Uluzzian	Equid	AF	38,000	900	0.00885	0.00103	-20.1
37247	bone	RSA" upper 12 F14 I	Uluzzian	Cervid	AF	37,500	900	0.00935	0.00104	-19.8
37246	bone	RSA" upper 12 F14 I	Uluzzian	Cervid	AF	38,500	1000	0.0083	0.00106	-19.4
39604	bone	RSA" upper 12 G14 IV	Uluzzian	Equid	AF	36,220	750	0.01101	0.00102	-20.3
37245	bone	RSA" upper 12 G14 IV	Uluzzian	Rupicapra	AF	37,800	900	0.00903	0.00102	-19.6
X-2733-13 ^a	bone	RPI lower 12 G13 II	Uluzzian	Bovidae/Cervidae/Giraffidae	AF	36,000	700	0.0113	0.00101	-19.7
X-2772-7 ^a	"	"	"	"	HYP	35,100	1100	0.01263	0.00176	-26.4
X-2698-46	charcoal	Base RSA"	Uluzzian	Not identified	YR	36,480	390	0.01067	0.00052	-25.7
37251	bone	RPI 13 G13	Uluzzian	Bovidae	AF	37,400	900	0.00947	0.00105	-19.2
37250	bone	RPI 13 G13	Uluzzian	Bovidae	AF	38,700	1000	0.00812	0.00106	-19.6
39605	bone	RPI upper 14 G13 II	Uluzzian	Cervid	AF	37,730	910	0.00912	0.00103	-19.6
37244	bone	RPI upper 14 G14 II	Uluzzian	Cervid	AF	39,300	1100	0.00748	0.00099	-19.3
37243	bone	RPI upper 14 G14 II	Uluzzian	Cervid	AF	38,600	1000	0.00817	0.001	-18.0
37252	bone	RPI upper 14 G13 II	Uluzzian	Cervid	AF	39,100	1100	0.00768	0.00101	-20.0
37254	bone	PIE lower 15 - upper 16 H14 I	Uluzzian	Equid	AF	38,600	1000	0.00818	0.00102	-20.2
37253	bone	PIE lower 15 - upper 16 H14 I	Uluzzian	Cervid	AF	38,600	1100	0.00818	0.00109	-20.2
37249	bone	RSI lower 16 H13 I	Uluzzian	Rupicapra	AF	38,500	1000	0.00828	0.00104	-19.1
37248	bone	RSI lower 16 H13 I	Uluzzian	Capra	AF	38,500	1000	0.00829	0.00102	-19.1
X-2733-15	bone	RSI lower 19 H14 III	Mousterian	Deer/Gazelle/Saiga	AF	40,500	1200	0.00647	0.00099	-20.1
X-2733-14	bone	RSI lower 20 F14 II	Mousterian	Ovidae/Cervidae/Giraffidae	AF	38,800	1000	0.00797	0.00101	-19.2
X-2733-12	bone	RSI lower 20 F12 I	Mousterian	Ovis/Capra	AF	39,600	1100	0.0072	0.00102	-19.2

^aDenote duplicate results from the same bone, but with different methods. Pcode denotes the pretreatment chemistry method applied. AF denotes samples treated using ultrafiltration of collagen. HYP denotes the sample dated using compound-specific hydroxyproline dating. YR denotes samples dated using the AOx-SC method. XR denotes samples dated using the ABOx-SC method. fM is the fraction modern carbon. These values were used in the calibration and modelling. Error terms are at ± 1 sigma. Oxa-22622 was previously published⁴⁰. Taglio is the Italian term for spit, a determined unit of stratigraphic depth used in excavation. Species identifications on bone were undertaken using ZooMS. See Supplementary Information for details of the analytical chemistry and stable isotopes.

Results

Radiocarbon dating

Radiocarbon determinations from Castelcivita, Cavallo, Cala and Oscurusciuto are reported in Tables 1–4, respectively. Analytical data associated with the radiocarbon AMS dates from the first three sites is given in the Supplementary Information (Supplementary Data 2–4). At Castelcivita, the application of %nitrogen analysis yielded a total of 19 samples of bone of which 16 produced acceptable collagen yields (Supplementary Data 1). Six of the bone AMS determinations later obtained were proportionally low in collagen (<1% wt.). These were given OxA-X- prefixes to alert the reader that their pretreatment chemistry was not ideal. We also AMS dated two fractions of one bone from spit 12 (Uluzzian rpi, G13II, lower 12), which were prepared using ultrafiltration and with the single amino acid hydroxyproline (HYP)⁵⁰. The statistical similarity between the two suggests that there is likely to be no significant contamination in the bulk bone collagen, although more comparisons would be needed if we were to extend this conclusion with confidence across all the bulk collagen dates.

Luminescence dating

The contexts of the luminescence ages are shown in Table 5 and the results in Table 6. At Castelcivita, all the age determinations are consistent with the depth and seem to cover only a few thousand years. The samples from the Mousterian layers gave similar ages at

48.6 ± 3.3 ka (CTC_X7030_SB13) and 47.0 ± 3.7 ka (CTC_X7030_SB12). The layer (rsi spit 18) at the boundary between the Mousterian and the Uluzzian (rsi spit 18) gave an age of 39.2 ± 3.1 ka (CTC_X7028_SB11). Three determinations for the Uluzzian layers range from 41.8 ± 2.4 ka, 39.5 ± 3.5 ka, and 37.9 ± 2.9 ka. The layer at the boundary between the Uluzzian and Protoaurignacian gave a result at 42.4 ± 2.8 ka, which remains coherent with the rest of the sequence at one sigma error. The following Proto- and Early Aurignacian layers gave three determinations at 42.4 ± 3.7 ka, 38.9 ± 2.9 ka and 36.7 ± 3.3 ka.

At Cala, all the age determinations are consistent with depth at one sigma. The five determinations from the Mousterian layers range from 74.9 ± 8.8 ka to 50.7 ± 5.5 ka. Four determinations from the Uluzzian layers range from 44.0 ± 4.4 ka to 40.2 ± 3.4 ka. One determination was obtained from the Aurignacian layer 36.6 ± 2.4 ka.

At the base of the Oscurusciuto excavated sequence, a tephra layer that has not been identified gave an age estimation of 66.0 ± 4.4 ka. Stratigraphic units 26, 24, and 19 gave age determinations at 66.8 ± 4.4 ka, 60.6 ± 3.3 ka, and 56.5 ± 4.4 ka, respectively. Stratigraphic unit 13 was dated at 66.6 ± 3.7 ka, coherent with the rest of the sequence at two sigma. In the subsequent stratigraphic units, the age determinations are coherent at one sigma and range from 52.0 ± 3.7 ka (stratigraphic unit 11) to 38.0 ± 2.3 ka (stratigraphic unit 3). The uppermost sample, in stratigraphic unit 2, gave a result of 39.8 ± 2.3 ka.

Table 2 | Radiocarbon dates from the site of Grotta del Cavallo

OxA/OxA-X-	Sample ID	Material	Species	¹⁴ C age BP	± error	fM	± error	δ ¹³ C (‰)
21072	Cvl 10	shell	<i>Cyclope neritea</i>	19,685	75	0.08627	0.00082	2.6
19254	Cvl 2	shell	<i>Tellina</i> sp.?	35,080	230	0.01269	0.00036	0.8
19255	Cvl 4	shell	<i>Antalis</i> sp.	36,260	250	0.01095	0.00035	2.1
20631	Cvl 11	shell	<i>Antalis</i> sp.	36,780	310	0.01027	0.00039	2.3
19257	Cvl 6	shell	Bivalve fragment	42,360	400	0.00513	0.00025	1.7
19258	Cvl 8	shell	<i>Antalis</i> sp.	36,000	400	0.01131	0.00057	2.5
19256 ^a	Cvl 5	shell	<i>Antalis</i> sp.	39,060	310	0.00773	0.0003	3.1
2280-16 ^a	"	"	"	38,300	400	0.00849	0.00042	3.1
40125 ^a	CAV12	charcoal	Not identified	40,400	1900	0.00653	0.00152	-24.2
40126 ^a	"	"	"	40,900	2100	0.006122	0.00161	-24.1
19242	Cvl 3	shell	<i>Antalis</i> sp.	39,990	340	0.00689	0.00029	3.3
40043	CAV11	charcoal	Not identified	38,150	450	0.00865	0.00048	-25.7
40124	CAV8	charcoal	Not identified	40,700	2100	0.00629	0.0016	-25.9
40042	CAV9	charcoal	Not identified	38,730	480	0.00805	0.00048	-23.7
40041	CAV7	charcoal	Not identified	38,450	470	0.00833	0.0005	-25.9
3070-15	CAV10	charcoal	Not identified	38,600	2200	0.00818	0.00226	-25.0
40040	CAV6	charcoal	Not identified	38,390	570	0.00840	0.00059	-25.7
40039	CAV5	charcoal	Not identified	39,540	590	0.00728	0.00053	-23.9
39973	CAV3	charcoal	Not identified	38,530	470	0.00825	0.00048	-23.6
39972	CAV1	charcoal	Not identified	38,110	580	0.00870	0.00063	-24.8
41397	CV698	bone	Bovid	38,300	1700	0.00846	0.00183	-19.3
3125-18	CV327	bone	<i>Equus</i>	37,600	1900	0.00929	0.00218	-21.1
3125-17	CV384	bone	Bovid	37,600	1700	0.00928	0.00194	-18.8
3125-16	CV326	bone	Artiodactyla	35,200	1200	0.01243	0.00184	-20.0
3125-9	CV632	bone	Artiodactyla	36,200	1400	0.01104	0.0019	-19.8

See caption for Table 1 for details. OxA-21072 was not included in the Bayesian model. The shell determinations were obtained by Douka⁵⁵. Species identifications were undertaken using ZooMS.

^adenotes duplicate samples.

Bayesian modelling

We built Bayesian models with the chronometric results for each site with OxCal 4.4 software⁵¹ and the IntCal20 and Marine20 calibration curves^{52,53} (see Supplementary Note 3 for methodological details).

The Bayesian model built for Castelcivita appears robust with few outliers (Fig. 3). All posterior outlier probabilities ranged between 4 and 10%. Convergence values averaged 98.9%. We were not able to confidently date the beginning of human occupation at the site due to the failure of samples at the base of the Mousterian to yield enough dateable carbon. The start of spit 24 (the earliest dated section of the site) is the earliest dated level and this ranges in age between 47,800–44,000 years cal BP (all ranges are given at 95% probability). The latest Mousterian is associated with spit 19 and a phase of semi-abandonment of the cave by humans from spit 18 up until the onset of the Uluzzian. Only 8 tools were identified within this spit. We obtained the highest posterior density (HPD) range of 43,850–43,070 years cal BP for the final Mousterian boundary.

The onset of the Uluzzian is estimated to start at 43,540–42,840 cal BP. With the end of spit 11, we observe the initial stage of the Aurignacian, the Protoaurignacian, as the Uluzzian gives way. Radiocarbon dates from here cluster tightly together, and the model estimates *a posteriori* range of 40,400–39,850 cal BP. The Aurignacian layers are capped by a series of flowstones containing interbedded tephra from the Campanian Ignimbrite (or Y-5 in the marine environment) eruption. Prior to this, in the sediment immediately preceding the CI, we obtained four OSL dates in sequence from spits 10, 9 (upper) (ProtoAurignacian), 6 (upper), and 4 (lower) (Early Aurignacian), which are entirely consistent with the ages below and with ages ascribed to the CI. An AMS determination from a fireplace in the Early Aurignacianic phase is in excellent agreement with the OSL dates. With the deposition of the tephra, the Aurignacian sequence ends, along with

this period of human occupation of the cave. Figure 4 shows the key boundaries in the Castelcivita model compared against the NGRIP δ¹⁸O curve⁵⁴.

The Cavallo age model includes shell determinations obtained previously^{15,40,55}, as well as new radiocarbon determinations on charcoal and bone from the key early Uluzzian level EIII (Fig. 5). These bones were screened using %nitrogen methods⁵⁶. The bones ranging from OxA-39972-41397 were identified as having reasonably intact collagen and subsequently dated. We aimed to date them using single amino acid analysis⁵⁰; however, the collagen content following extraction was too low, and they were dated using the ultrafiltration protocol instead. For marine shell determinations, we used an undefined marine reservoir correction (or Delta_R) value (Delta_R(" - Undefined Local Marine", U(-500, 500))). Usually, we would apply a Delta_R value using Reimer and Reimer⁵⁷, along with the Marine20 calibration curve⁵², but the samples are extremely old and there are several assumptions involved, particularly in terms of temporal change in the local reservoir. We, therefore, allowed the Delta_R value to float, enabling the model to define the most likely value. Once again, the C_Date command was used to include the tephra Ar/Ar dates for the Y-6 and Y-5 ash layers. The Y-6 tephra sits³⁶ towards the base of the model and marks the end of the Mousterian at Cavallo. Below it, we included two determinations from the Firenze laboratory⁵⁸. We left OxA-21072 out of the model because it is a significantly underestimated result.

The EIII Uluzzian level is dated by eight AMS dates, five of which have some caveats in addition to higher-than-ideal standard errors. The four determinations denoted with OxA-X- prefixes had proportionally low collagen yields, ranging between 0.3 and 0.4%. A fifth determination (OxA-41397) gave a lower-than-expected carbon content on combustion (16.6%). This radiocarbon determination should be

Table 3 | Radiocarbon AMS dates from the site of Cala, along with details of samples that failed to be AMS dated

P number	OxA	Context comment	Sample ID	Layer	Material	Species/ZoMS	^{14}C age BP	\pm error	$\delta^{13}\text{C}$ (‰)	%N	%C
41993	Failed, low yield	Bone selected from R, immediately below the β level.	1 R Internal	R Internal	bone	no ID	-	-	0.03	-	-
41994	Failed, low yield	Charcoal from top of 6, or β ? within stalagmite	2 Internal top of 6	Interna top of 6	charcoal	no ID	-	-	-	-	-
41995	Failed, low yield	Bone from Q lower just above β	3 Internal Q lower just above β	Internal Q lower just above β	bone	no ID	-	-	0.05	-	-
41996	Failed, low yield	Bone from lower part of level Q	4 Internal Q lower	Internal Q lower	bone	no ID	-	-	0.09	-	-
41997	35427	Charcoal from internal section, this is from Q. Careful cleaning required, lots of rootlets seen.	5 Internal from Q mid	Internal from Q mid	charcoal	no ID	26,230	150	-24.0	79.1	-
41998		Sample associated with charcoal sample number 5.	6 Internal from Q lower/middle	Internal from Q lower/middle	bone	Deer/Gazelle/Saiga	-	-	-	-	-
		Failed, low yield	Sample associated with charcoal sample number 5.	6 Internal from Q lower/middle	Internal from Q lower/middle	bone	Deer/Gazelle/Saiga	-	-	-	-
41999	35601	Sample of charcoal associated with bone sample 6	7 Internal level Q mid-lower	Internal level Q mid-lower	charcoal	no ID	26,030	370	-23.8	16.6	-
42000	35428	Sample of charcoal from Q upper	8 Internal Q upper	Internal from Q upper corner	charcoal	no ID	26,280	150	-22.0	71.9	-
42001	Failed, low yield	Sample of bone associated with sample 8, from upper corner of Q	9 Internal Q upper corner	Internal Q upper corner	bone	no ID	-	-	0.03	-	-
42002	35429	Charcoal from upper Aurignacian	10 Atrio Aurignacian	Sq C7, charcoal Aurignacian	charcoal	no ID	33,410	320	-23.6	-	81.3
		Species identifications were undertaken using ZoMS.									

interpreted as a minimum age. We observe that a sixth determination, OxA-39972, a charcoal date treated with oxidation and stepped combustion approaches, gave an age of $38,110 \pm 580$ BP. These methods yield reliable AMS dates, so we see this measurement as accurate.

The model shows good agreement between the tephra ages and the radiocarbon results. There were three notable outliers. OxA-19257, a shell determination from phase DII¹⁵ yielded a posterior outlier probability of 100% and was, therefore, down-weighted in 100% of the runs of the model and can be discounted as an influence on the results of the Bayesian model. One of the bone determinations from EIII gave an elevated posterior outlier probability (49% for OxA-X- 3125-16). Future work will focus on attempting to date larger and better-preserved bone or teeth samples from this key level to explore whether there are any significant age shifts from what we have obtained in this paper. For the time being, we conclude that the age of the earliest Uluzzian is at least $42,650\text{--}42,150$ cal BP at Cavallo but not older than $45,000 \pm 1000$ cal BP; that being the age of the Y-6 tephra, which acts as a *terminus post quem* in the model (*c.f.* ref. 36).

Grotta della Cala was a challenging site to date. We tested several bone samples using %nitrogen methods (Table 3) but, unfortunately, these were all very low (range 0.03–0.09% N), indicating no significant collagen or protein remaining. We also selected charcoal samples for analysis. One significant result we obtained was a date for a sample of charcoal from a concentration found in square C7 just below a hearth feature in that area. This sample belongs to the uppermost Aurignacian in the Cala Atrio sequence and sits in good agreement stratigraphically above an OSL date (X7042) that comes from spit 12 (Table 6). Together, the results suggest that the Aurignacian at Cala begins at $42,050\text{--}37,400$ cal BP (95.4%), in broad agreement with the transition from the Uluzzian to the Protoaurignacian at Castelcivita. The Cala model is, however, affected by poor precision *a posteriori* (Fig. 6). Despite this, our results show that the Uluzzian is not as young as once seemed based on previous radiocarbon determinations; the Late Mousterian to Uluzzian sequence now sits temporally between $45,000\text{--}40,000$ cal BP, rather than later. We estimate the start boundary of the Uluzzian here is $45,150\text{--}40,400$ cal BP (at 68.3% prob.). This is consistent with the pattern established at the other sites, which are better dated.

At Oscurusciuto, we obtained ten OSL dates and a single AMS determination (Fig. 7). Radiocarbon was again challenging due to the absence of recoverable charcoal from the sequence and the lack of collagen in any of the bones from the site. One sample of charcoal from stratigraphic unit 11 failed to yield any recoverable carbon after pre-treatment. We included previous K-Ar dates from Mount Epomeo Green Tuff in stratigraphic unit 14⁴⁷ in the Bayesian model we built. The OSL dates above them fall in their correct age order. One OSL measurement (X7050) is an outlier (86%), deemed to be too old for its position in stratigraphic unit 13. It is placed stratigraphically above the Mount Epomeo Green Tuff dates, which all cluster at 55,000 cal BP, so much depends on their reliability in terms of the outlier value detected for X7050. More work is needed. The previously obtained Beta Analytic AMS data that comes from the stratigraphic unit also has a 49% outlier probability. The sole AMS date we obtained came from stratigraphic unit 1 but yielded a “greater than” age ($>41,600$ BP) due to a lower-than-expected value for carbon on combustion. It is justifiably a minimum age, and we do not include it in the Bayesian model. Taken together, the Oscurusciuto model provides a robust sequence for the Mousterian at this important site. The absence of transitional layers (Uluzzian and Protoaurignacian) limits its importance in discussing the bio-cultural shift from Neanderthals to modern humans in this part of the world, however. In addition, the precision of the age estimates for the final Mousterian limits its importance in exploring the dates by which Neanderthal populations had disappeared in Italy (the age range for the end of stratigraphic unit 1 covers $42,950\text{--}34,400$ cal BP at 95.4% prob., although the distribution for the end of stratigraphic unit 3 is bimodal, with most of the distribution sitting prior to 40,000 cal

Table 4 | AMS radiocarbon dates from Oscurusciuto

P number	OxA	Context comment	Sample ID	Layer	Material	¹⁴ C age BP	$\delta^{13}\text{C}$ (‰)	%C
41991	35600	Topmost tephra layer	Sample 1	Layer 13	Charcoal	>41,600	-24.8	7.9
41992	FAIL	Sample of charcoal from layer 11	Sample 2	layer 11	Charcoal	-	-	-

Table 5 | Sample identifications and context details of the sediments OSL dated

Sample ID (Site sampledID_Oxford_sampleID_StonyBrook)	Layer	Location
CTC_X7021_SB4	ARS (Early Aur)	Z: -0.40 m = 4 lower
CTC_X7022_SB5	ARS (Early Aur)	Z: -0.51 m = 6 upper
CTC_X7023_SB6	RSA' (Protoaur)	Z: -0.85 m = 9 upper
CTC_X7024_SB7	RSA/RSA'' (Protoaur/UL)	Z: -0.95 m = 10 upper
CTC_X7025_SB8	RPI (UL)	Z: -1.20 m = 12 lower
CTC_X7026_SB9	RPI/PIE (UL)	Z: -1.31 m = 14 upper
CTC_X7027_SB10	PIE/RSI (UL)	Z: -1.48 m = 15 lower
CTC_X7028_SB11	RSI (UL)/RSI (Moust)	Z: -1.73 m = 18 upper
CTC_X7029_SB12	RSI base (Moust)	Z: -2.06 m = 21 upper
CTC_X7030_SB13	GAR (Moust)	Z: -2.40 m = 24 lower
CALA_X7043 ^a	Aurignacian 11	Atrio series, Square E8
CALA_X7042_SB15	Aurignacian 12	Atrio series, Square E8
CALA_X7041_SB16	Uluzzian 14	Atrio series, Square E8
CALA_X7036_SB21	Uluzzian top	Atrio series, Square D6
CALA_X7035_SB22	Uluzzian middle	Atrio series, Square D6
CALA_X7034_SB23	Uluzzian base	Atrio series, Square D6
CALA_X7033_SB24	Mousterian	Atrio series, Square D6
CALA_X7040_SB17	Mousterian R	Internal series, Square E/D15
CALA_X7039_SB18	Mousterian S	Internal series, Square E/D15
CALA_X7038_SB19	Mousterian T	Internal series, Square E/D15
CALA_X7037_SB20	Mousterian T	Internal series, Square E/D15
OSC_X7044 ^a	SU 1	Square H9; X: 30; Y: 80; Z: -0.90 m
OSC_X7045_SB25	SU 2	Square H9; X: 20; Y: 90; Z: -1.30 m
OSC_X7046_SB26	SU 3	Square H10; X: 20; Y: 70; Z: -2.00 m
OSC_X7047_SB27	SU 4	Square H10; X: 20; Y: 90; Z: -2.28 m
OSC_X7048_SB28	SU 7	Square H11; X: 20; Y: 10; Z: -2.50 m
OSC_X7049_SB29	SU11	Square H11; X: 20; Y: 10; Z: -2.70 m
OSC_X7050_SB30	SU 13	Square H11; X: 20; Y: 20; Z: -2.80 m
OSC_X7051_SB31	SU 19	Square D15; X: 60; Y: 90; Z: -3.80 m
OSC_X7052_SB32	SU 24	Square D16; X: 20; Y: 90; Z: -4.02 m
OSC_X7053_SB33	SU 26	Square D16; X: 60; Y: 90; Z: -4.16 m
OSC_X7054	Base tephra layer	n.d.

^aSamples did not contain datable quartz coarse grains after chemical treatment.

BP). For these reasons, the Oscurusciuto site is not discussed further in the synthesis of the results below.

Discussion

The results presented in this paper represent the most extensive dating study yet of the Uluzzian and wider Middle to Upper Palaeolithic succession in Italy. The highest posterior distributions (HPDs) from important transitions in the different models we constructed can be compared to explore spatio-temporal patterns and answer questions of contemporaneity and first/last appearances of the different technocomplexes under study. Throughout this discussion we assume that the Mousterian technocomplex is exclusively related to Neanderthals and that the Uluzzian and Protoaurignacian are linked only with modern humans.

First, we compare HPDs from the final Mousterian boundaries. The analysis includes Cavallo and Castelcivita, as well as other Italian sites previously dated, including Riparo Mochi⁵⁹, Grotta di Fumane^{6,60}, Grotta di Rio Secco⁶¹, Riparo Broion⁶² and Grotta Reali⁶³ (Fig. 8). Taken together, the results, based on tens of AMS determinations, appear in close agreement and are robust. We observe a high degree of overlap and similarity, which suggests that by ~43,000 cal BP the Mousterian had ended along the length of the peninsula, although at some sites (e.g., Rio Secco), the Mousterian occupation had seemingly ended significantly prior to this. The results strongly suggest a broadly contemporary end date for the Italian Mousterian (or abandonment of these sites by Neanderthals).

At Cavallo, the Y-6 tephra in layer Fa represents a well-defined *terminus ante quem* for the abandonment of the cave by Neanderthals. This thin layer overlies the last Mousterian layer FI, separating it from layer Fs, which constitutes the base of the Uluzzian occupation. Stratigraphically, the chronological interval between the Late Mousterian and the Uluzzian corresponds to a depositional hiatus in sedimentation (see Supplementary Note 1). The dates from layer EIII suggest that the inception of the Uluzzian at Cavallo may have been younger than previously determined¹⁵ and thereby provide further confirmation of the stratigraphic evidence. This suggests that the Neanderthals left the site, and perhaps the wider area, prior to the arrival of *H. sapiens* represented by the Uluzzian. This can be tested with more well-dated and Bayesian-modelled sites, but on present evidence, it seems a robust conclusion. We calculated a probability distribution for the final Mousterian across the peninsula using the method of Higham et al.⁶⁰, treating the individual model boundaries as prior distributions within a Phase. This yielded a final Mousterian HPD of 43,700–41,850 cal BP (at 95.4% prob.) (Fig. 8).

Next, we turn to the parts of the models representing the start boundaries for the Uluzzian and Protoaurignacian industries. These are summarised in Fig. 9. Only three Uluzzian HPDs are included. Although recent dates are available also from the Middle to Upper Palaeolithic deposit of Rocca San Sebastiano (Mondragone, Campania), these were not considered due to the identification of some mixing inside the Uluzzian layer of this site^{22,64}. At Grotta di Fumane, in the A3 phase, some degree of post-depositional disturbances *ab antiquo* has also been recognised^{7,32,65}, possibly caused by activities carried out by the Protoaurignacian inhabitants of layer A2. Chronological data from this level must, therefore, be treated with caution, at

Table 6 | OSL measurements, doses and ages of the sediment samples from Castelcivita, Grotta della Cala and Oscurusciuto

Sample ID	Layer	"Oxford" ^a / ^b "StonyBrook" ^a	De (Gy) ^b	OD (%) ^b	OSL age (ka) ^c
CTC_X7021_SB4	ARS(EA)	6 + 7	131.88 ± 9.18	19 ± 4	36.7 ± 3.3 (2.8)
CTC_X7022_SB5	ARS(EA)	3 + 12	112.89 ± 5.88	16 ± 3	38.9 ± 2.9 (2.2)
CTC_X7023_SB6	RSA'(P)	3 + 5	123.81 ± 7.70	16 ± 4	42.4 ± 3.7 (3.0)
CTC_X7024_SB7	RSA'(P)/RSA"(U)	3 + 9	121.98 ± 4.22	10 ± 2	42.4 ± 2.8 (2.0)
CTC_X7025_SB8	RPI(U)	10 + 5	104.84 ± 5.83	16 ± 3	37.9 ± 2.9 (2.2)
CTC_X7026_SB9	RPI/PIE(U)	5 + 6	110.89 ± 8.07	21 ± 5	39.5 ± 3.5 (3.0)
CTC_X7027_SB10	PIE/RSI(U)	0 + 12	114.21 ± 3.01	8 ± 2	41.8 ± 2.4 (1.3)
CTC_X7028_SB11	RSI(U)/RSI(M)	3 + 9	105.34 ± 6.07	19 ± 5	39.2 ± 3.1 (2.4)
CTC_X7029_SB12	RSI(M)	4 + 27	97.03 ± 5.70	31 ± 4	47.0 ± 3.7 (3.0)
CTC_X7030_SB13	GAR(M)	4 + 19	127.48 ± 4.13	14 ± 2	48.6 ± 3.3 (2.1)
CALA_X7042_SB15	A	7 + 10	49.1 ± 2.33	17 ± 4	36.6 ± 2.4 (1.8)
CALA_X7041_SB16	U	6 + 13	94.99 ± 6.72	30 ± 5	40.2 ± 3.4 (2.9)
CALA_X7036_SB21	U top	4 + 2	46.72 ± 4.95	20 ± 8	40.8 ± 4.8 (4.4)
CALA_X7035_SB22	U middle	3 + 4	43.62 ± 6.44	25 ± 11	36.9 ± 5.6 (5.1)
CALA_X7034_SB23	U base	3 + 0	52.6 ± 4.8	20 ± 9	44.0 ± 4.4 (4.1)
CALA_X7033_SB24	M	6 + 0	67.72 ± 4.6	0	56.8 ± 4.5 (4.0)
CALA_X7040_SB17	Layer R (M)	7 + 2	84.32 ± 4.13	12 ± 4	50.7 ± 5.5 (2.6)
CALA_X7039_SB18	Layer S (M)	8 + 14	119.6 ± 7	26 ± 4	62.0 ± 6.4 (3.8)
CALA_X7038_SB19	Layer T (M)	6 + 9	146.5 ± 11	26 ± 6	74.9 ± 8.8 (6.0)
CALA_X7037_SB20	Layer T (M)	7 + 5	171.12 ± 11.8	21 ± 5	70.5 ± 7.5 (5.1)
OSC_X7045_SB25	SU 2	5 + 23	86.43 ± 3.00	18 ± 3	39.8 ± 2.3 (1.6)
OSC_X7046_SB26	SU 3	5 + 10	105.77 ± 4.24	15 ± 3	38.0 ± 2.3 (1.7)
OSC_X7047_SB27	SU 4	6 + 8	133.41 ± 4.59	11 ± 3	45.6 ± 2.6 (1.8)
OSC_X7048_SB28	SU 7	7 + 24	111.68 ± 3.18	15 ± 2	41.9 ± 2.2 (1.5)
OSC_X7049_SB29	SU 11	4 + 32	104.85 ± 2.69	16 ± 2	52.0 ± 3.7 (2.1)
OSC_X7050_SB30	SU 13	3 + 25	163.24 ± 5.53	17 ± 2	66.6 ± 3.7 (2.6)
OSC_X7051_SB31	SU 19	6 + 24	95.26 ± 3.60	20 ± 3	56.5 ± 4.4 (2.7)
OSC_X7052_SB32	SU 24	21 + 11	81.50 ± 2.15	14 ± 2	60.6 ± 3.3 (2.0)
OSC_X7053_SB33	SU 26	21 + 8	70.87 ± 2.67	20 ± 3	66.8 ± 4.4 (2.9)
OSC_X7054	Base tephra layer	15 + 0	88.90 ± 4.04	17 ± 3	66.0 ± 4.4 (3.2)

^a'noxford' is the number of aliquots measured at the Oxford laboratory, '^bstonybrook' is the number of aliquots measured at the Stony Brook laboratory. ^bEquivalent dose (De) and overdispersion (OD) were calculated using the central age model (Galbraith et al., 1999). ^cAges are reported in 10³ years (ka), and the uncertainty shown after the ± symbol is the quadratic sum of the random and systematic uncertainties at 1σ; values shown in brackets are the random-only errors (used for Bayesian modelling purposes). EA early Aurignacian, P Protoaurignacian, U Uluzzian, M Mousterian.

least until a thorough taphonomic and geoarchaeological revision of A3 assemblage is performed and new AMS and OSL age estimates are published.

We used the Order command in OxCal to determine the most likely order of events in the boundaries for the models built (Supplementary Data 7). At Castelcivita, the start of the Uluzzian coincides with the end of the Mousterian, so the distributions are the same. Our analysis shows that the Uluzzian at Castelcivita is earlier than at Cavallo (97.9% prob.), supporting the idea above of a gap in the Uluzzian occupation of Cavallo by *H. sapiens* following abandonment by, or disappearance of, Neanderthals. Alternatively, the earliest Uluzzian at Cavallo, which is so far not exhaustively dated, represents a slight underestimate of the real age.

We also compared the results with the Riparo Broion⁶² (Fig. 9). We found that the Uluzzian of Castelcivita was 77.1% likely to have started prior to the same phase in Broion, although the latter is less well-dated and more work is undoubtedly needed.

Overall, our modelling results suggest that the Uluzzian did *not* begin synchronously in the northern and southern parts of the peninsula. The current data suggests it appeared first in the south, although we caution that data from the north remains limited.

Another important question is whether there is any spatio-temporal pattern in the dispersal of the Protoaurignacian in the

Italian Peninsula. Several scholars have suggested the potential movement of this technocomplex from north to south^{7,18}, but there has never been sufficiently good enough data to test this. To explore this further, we compare HPDs for the Protoaurignacian from Fumane, Mochi, and Castelcivita (we left out Cala due to the imprecision of its HPD region) (Fig. 9). We observe a cline in the HPDs, such that the earliest HPD from Mochi appears in the north and then significantly later, in the south, at Castelcivita. In statistical terms, the Protoaurignacian HPD from Mochi is significantly earlier than Castelcivita. Our Order analysis confirms that Mochi is 98.9% likely to pre-date Castelcivita and Fumane is 68.1% likely to pre-date Castelcivita. This suggests that the Protoaurignacian begins in the north, earlier, and then appears later in the south. Interestingly, the data also shows that in the south of the peninsula the Uluzzian persists, in the absence of the Protoaurignacian, until much later. This agrees with previous observations of modelled data from these sites⁴⁰. At Castelcivita, for example, where the record is the most reliable, the Uluzzian/Protoaurignacian boundary is 41,770–39,940 cal BP.

We also used the Date command to explore the total range in the dates for the three main technocomplexes across all sites. These are shown in Fig. 10. The results essentially support what we observed above. There is a degree of overlap between the earliest Protoaurignacian in the north of Italy with the latest Uluzzian in the south.

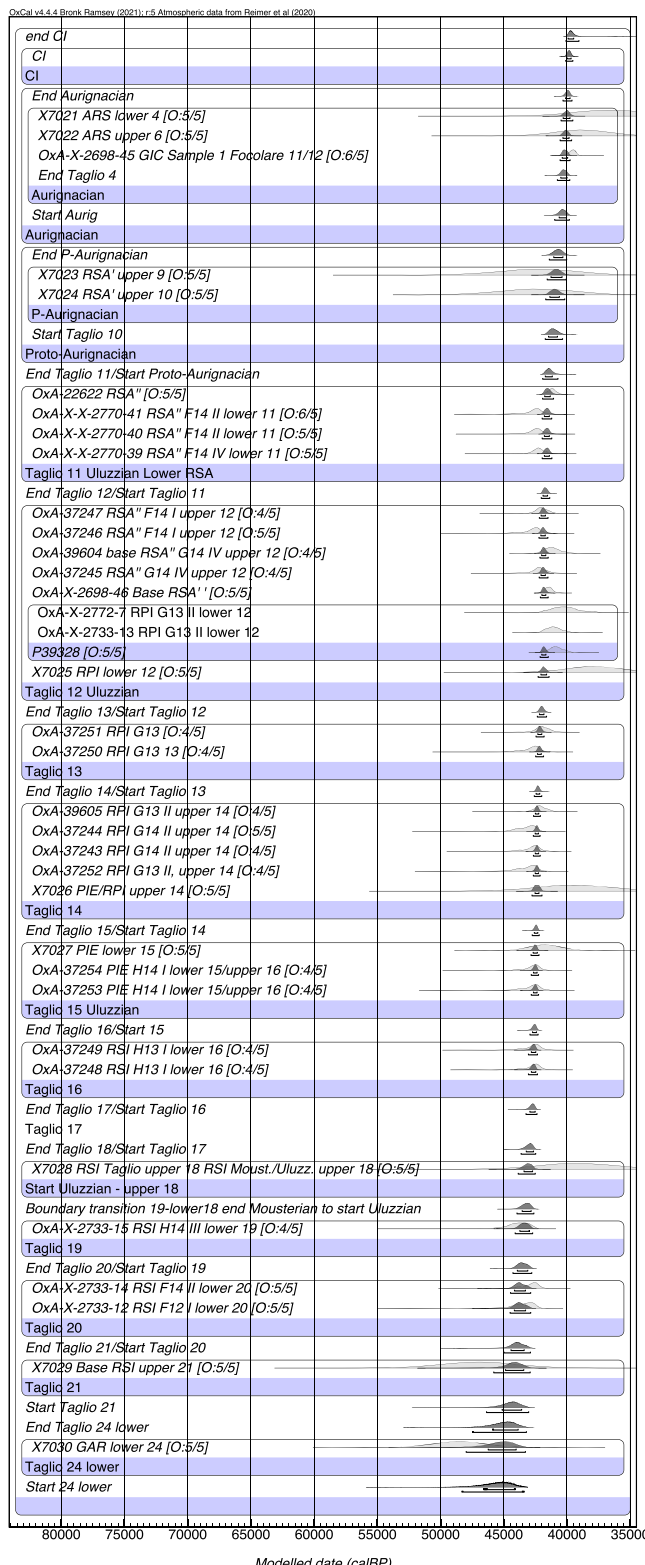


Fig. 3 | Bayesian age model from the site of Castelcivita. The model is made up of a Sequence of Phases in OxCal4.4.3. The Supplementary Code 1 attached to this paper contains the CQL code for all models. Radiocarbon determinations are given in fraction Modern (FM) (`R_F14C` notation in OxCal). N X- prefixed data are OSL dates with only random error terms included. `C_Date` denotes a Calendar Age and corresponds with the age of the CI Tephra. Duplicate measurements are combined using the `R_Combine` command. Outliers are shown in the figure in the form (O: posterior/prior). There are no significant outliers in this model. Note that Taglio refers to Spits (see text for details).

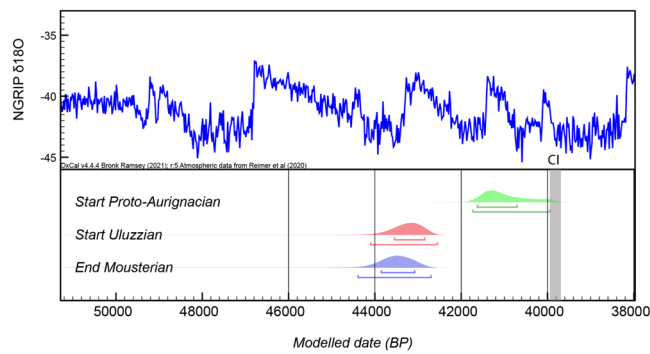


Fig. 4 | The key boundaries from the Castelcivita age model. The CI marks the age of the Campanian Ignimbrite tephra, based on the Ar-Ar age of Giaccio et al. (2017). The NGRIP oxygen isotope record is included for tentative comparison (Svensson et al., 2008).

We compare the date ranges with models built using the `KDE_Model` (Kernel Density Estimate) approach in OxCal⁶⁶ (Fig. 10). The `KDE_Model` results show that across Italy the Uluzzian centres just prior to 42,200 cal BP from 43,120–41,370 cal BP (at 68.2% prob.) and 44,580–39,790 cal BP (at 95.4%). Our study also allows us to constrain the length of the Uluzzian within more precise chronological limits, showing that this technocomplex lasted just over 2000 years in total, prior to the makers of the industry being assimilated/replaced by bearers of the Protoaurignacian technocomplex, as is hinted by the occurrence of Aurignacian-like lithic elements (marginally backed bladelets, Aurignacian blades, carinated artefacts and unretouched bladelets from lamellar production strategies) at Cala and in layers D of Cavallo and rsa" of Castelcivita^{7,43,67}.

A chronostratigraphic gap between the Late Mousterian and the Uluzzian is supported by the techno-typological characteristics of the Uluzzian lithic suite in which no filiation from the Mousterian is discernable⁷. Defining relationships between the Uluzzian and the Aurignacian is more challenging because data from the stratigraphic record and the lithic industry seem, in some cases, to conflict. We have evidence of a sedimentological discontinuity in sites like la Fabbrica and La Cala, but by contrast, we note the occurrence of Aurignacian-like lithic elements in the latest Uluzzian layers of Cavallo, Cala and Castelcivita, which could hint at cultural interactions and perhaps an assimilation process of the Uluzzian by the Protoaurignacian, instead of a mere replacement. The assimilation process is further supported by the frequent adoption of bipolar technology, a prominent characteristic of the Uluzzian, in the subsequent Proto and Early Aurignacian phases in southern Italy. Interestingly, bipolar technology is notably scarce or even absent in Aurignacian sites across northern Italy⁶⁷. To date, sites containing the Uluzzian–Protoaurignacian succession are too few to provide a reliable picture, and it is possible that both replacement and assimilation could be considered valid at a local scale.

To help visualise the data, we built spatio-temporal maps (Fig. 11), which show the distribution of the KDE timespans for the various industries across time and space.

Moroni et al.^{68,69} proposed two potential migration routes for humans bearing Uluzzian technology into the peninsula. The first route suggested a direct passage across the Otranto channel, from Greece to Apulia, while the second proposed a path along the Adriatic coast of the Balkans, crossing just above the Conero Promontory (south of modern-day Ancona) during MIS3 and spreading from there. The Otranto route, despite the challenges of sea crossings, was considered to harmonise with the initial emergence of the Uluzzian in Apulia ~45,000 years ago, which the dating then showed.

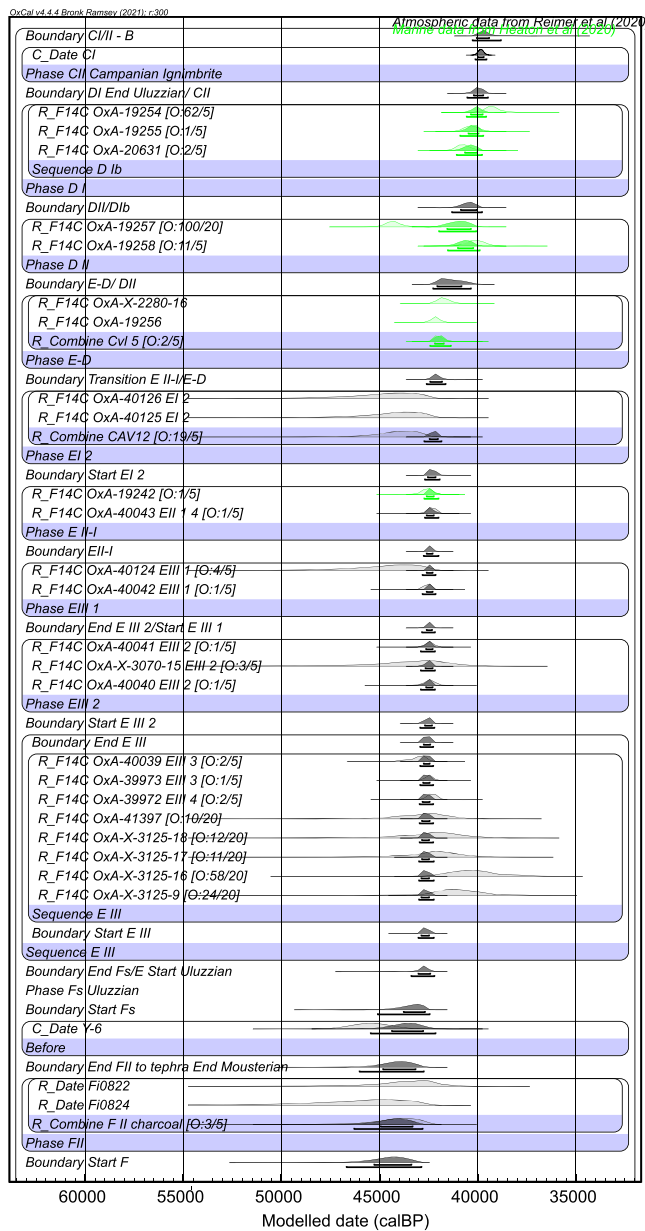


Fig. 5 | Bayesian age model from the site of Cavallo. Green posterior probability distributions are determinations of marine shells. Outlier probabilities (O: posterior/prior) are given next to the date information. We increased the prior outlier probability for the bone determinations from EIII to 20%. There is one outlier of significance over and above this threshold (OxA-X-3125-16 at 58%) at this level. See text for details and caption to Fig. 3.

The chronometric data presented here appears to favor the Otranto route, but we cannot rule out the possibility of two different dispersal pathways, and we remain open to the possibility that more data from the north (e.g., Fumane) might change the picture significantly.

A different scenario emerges, however, regarding the dispersal of the Protoaurignacian. This industry appears first in the northwest of the peninsula at the Riparo Mochi site, ca 42,000 years ago, at a time when the Uluzzian still persisted in the south. The delayed appearance of the Protoaurignacian is particularly evident at Castelcivita, and notably at Cavallo, where Protoaurignacian layers are entirely absent. Although possible evidence of Protoaurignacian occupations, stratigraphically overlapping the Uluzzian deposit, has been identified at the nearby site of Serra

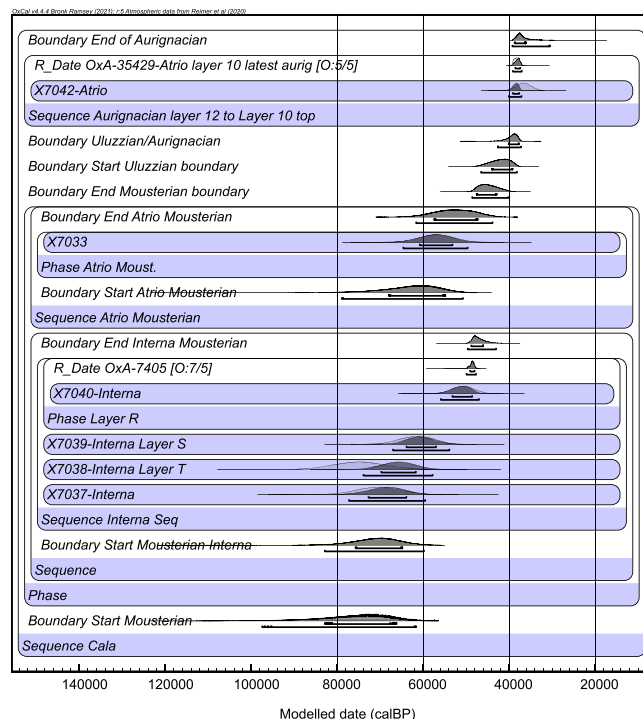


Fig. 6 | Bayesian model from Grotta della Cala. See text for details and caption to Fig. 3.

Cicora, the absence of chronological and revised archaeological data there poses a challenge^{70,71}.

The temporal overlap of Uluzzian and Protoaurignacian groups raises questions regarding whether these industries were made by a single human population, or different groups. Recent genetic evidence for the earliest *Homo sapiens* groups in Europe from sites such as Peștera cu Oase, Bacho Kiro, Zlatý kůň, and Ust-Ishim has shown that there were several distinct populations of modern humans across the early Upper Palaeolithic of Eurasia^{72–75}. Hajdinjak et al.⁷⁴ have suggested that successive waves of population replacement might have occurred during the Middle to Upper Palaeolithic in Europe (see also Vallini et al.⁷⁵). It is possible that the Uluzzian and Protoaurignacian industries in the Italian Peninsula might too have been produced by different human populations. Alternatively, they may reflect variations in the adaptative strategies of a single human population across different geographical regions. Finally, the coexistence of mixed groups or hybrid populations cannot be ruled out. The recovery of ancient DNA from human remains found in Uluzzian contexts would be a key step in resolving these alternatives and exploring the intricate dynamics of human migrations and cultural exchanges during this period⁷⁶.

Summing up, in this work we have obtained a suite of AMS and OSL determinations from four archaeological sites in Italy dating to the Middle to Upper Palaeolithic period. Bayesian models show strong convergence and robust results, with few, if any, outliers of significance. AMS and OSL chronometric results harmonise in excellent agreement, something that is not often seen in archaeological dating⁷⁷. The results allow us to compare key boundaries in the models marking the end of the Mousterian, as well as the start dates of the Uluzzian and Protoaurignacian across the Italian Peninsula and thereby interpret a fine-grained chronology. We observe that there is a broad synchronicity in the date estimates for the disappearance of the Mousterian. The date of the earliest Uluzzian is somewhat younger than previously seen⁶⁰, due mainly to the updated IntCal20 calibration curve⁵³. Rather than starting shortly after ~45,000 cal BP, as previously suggested^{40,60},

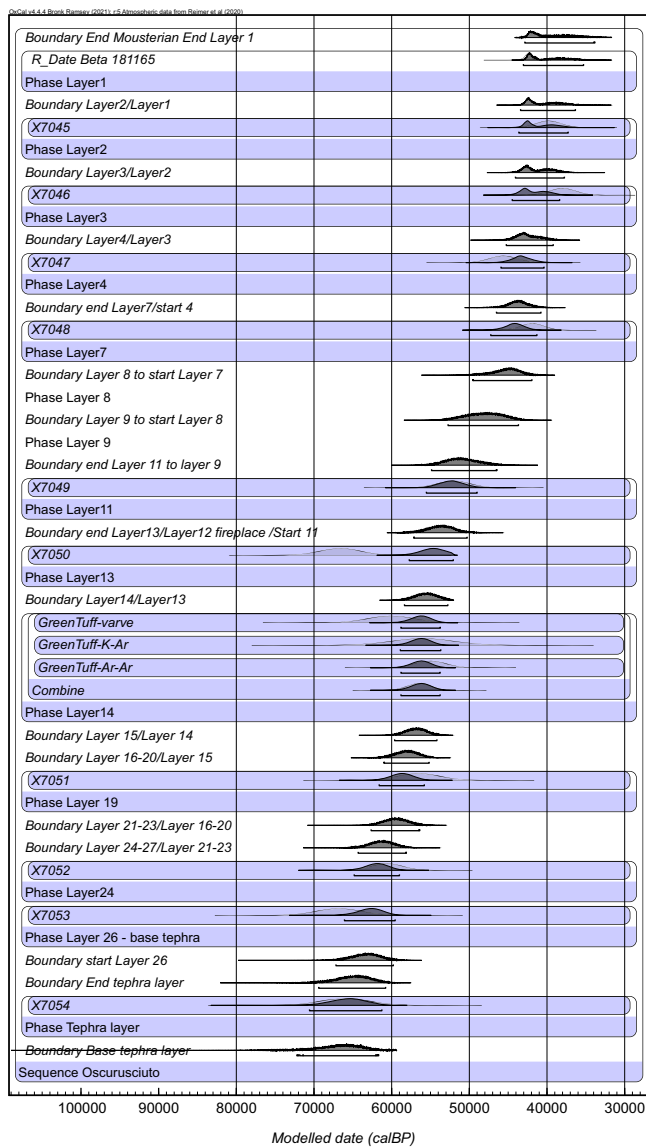


Fig. 7 | Age model from the site of Oscurusciuto. See text for details and caption to Fig. 3.

it dates instead from 43,120–41,370 cal BP (at 68.2% prob.) and 44,580–39,790 cal BP (at 95.4%). Although data is limited, the results suggest a slightly earlier emergence of the Uluzzian in the south. This despite the significant homogeneity and strong identity of the Uluzzian across Italy and Greece in terms of the material culture and ornaments identified^{18–20,25}. There is a hint that in Uluzzo Bay there is a slightly later onset, but this may be masked by challenges with the dating of the earliest EIII levels at Cavallo. This is something that we continue to work on. We also see evidence that there may have been a reduction in Neanderthal populations—in the sense that they most probably left the area—prior to the spread of the Uluzzian in the region. At Cavallo, for example, the Uluzzian occupation commenced only after the deposition of the Y-6 tephra, providing a *terminus post quem* for the start of this technocomplex. The wider evidence suggests that early *Homo sapiens* groups dispersing into the Italian Peninsula around 42,500 years ago probably encountered few, if any, local Neanderthals.

Methods

Permission and support for fieldwork in Apulia and Campania was obtained from the Soprintendenza Archeologia, Belle Arti e Paesaggio per le Province di Salerno e Avellino, Soprintendenza Archeologia,

Belle Arti e Paesaggio per le Province di Brindisi e Lecce and Soprintendenza Nazionale per il Patrimonio Culturale Subacqueo. Excavations were conducted under permission of MiC (MIC|MIC_DG_ABAP_SERV II_UO1|07/06/2021|0019224-P| [34.61.07/1.15.1/2019]; MIC|MIC_DG_ABAP_SERVII|30/09/2021|0032649-P| [34.61.07/1.14.1/2019] and DG-ABAP 20/06/2022 decreto 809). Please see Supplementary Note 2 for excluded sites.

Three main factors make the radiocarbon dating part of this project possible. First, the publication of the new IntCal20 calibration curve extends the range of calibration back to 55,000 cal BP⁵³. IntCal20 has higher resolution data, particularly for the earlier parts of the timescale, and was constructed using a new statistical method⁷⁸, enabling improved comparison against climate and other independent records⁷⁹. Second, state-of-the-art sample preparation approaches for both radiocarbon and OSL, as well as increased AMS measurement precision, have enabled significant improvements over existing chronologies^{6,50}. Thirdly, the application of Bayesian modelling has had major impacts for both radiocarbon-specific models, as well as those including other methods, such as OSL, and cross-linked with tephra markers (as shown here). Chronometric models enable higher precision chronologies to be built, as well as inform us of the likelihood of outlying determinations.

Radiocarbon and luminescence dating methods were used at Castelcivita, Cala, and Oscurusciuto, while only radiocarbon dating was possible at Cavallo. Based on the results obtained, Bayesian models were built.

Radiocarbon dating

All radiocarbon dating was undertaken at the ORAU at the University of Oxford, UK. We used several methods to pretreat the samples prior to radiocarbon dating. For charcoal samples, we applied oxidation/stepped combustion methods. Charcoal was chemically pretreated using a variation of the usual acid-base-wet oxidation/stepped combustion (AOx-SC) protocol we employ for dating ancient Palaeolithic charcoal^{80,81}. A modified protocol (AOx-SC) eliminates the base step⁸². These methods have been shown to remove contaminants from Palaeolithic-aged charcoal much more efficiently than the routine acid-base-acid (ABA) protocols, with less sample loss. We have observed that AMS dates of these materials using this type of approach are often significantly older^{5,39,80,83–88}.

Bone samples were AMS-dated using the ORAU protocol for bone collagen extraction⁸⁹. The ultrafilters were pre-cleaned before use⁹⁰. We also used a single compound approach (targeting HYP) from a limited number of samples⁵⁰.

At Cavallo, samples were collected from a small trench excavation (50 × 30 cm) carried out in 2019 in the undisturbed Uluzzian deposit (Supplementary Information Fig S1). Shell carbonates from the Cavallo site (Gambassini's excavations) were treated prior to AMS dating using the methods outlined in ref. 15.

At Castelcivita, we undertook field and laboratory-based sampling of carbonaceous material for the radiocarbon part of the project. We sampled in the field from the current excavations of the Aurignacian areas of the site, as well as from the main section (for Protoaurignacian, Uluzzian, and Moustierian). Four samples were directly taken from a hearth in layer gic (squares L11-L12), which was recently attributed to an Early Aurignacian phase⁹¹. We identified samples of charcoal and bone from beneath the flowstone levels of the main section, down to -220 cm below the datum. Unfortunately, a total of 14 samples failed to yield any radiocarbon dates due to low or no carbon yields after pretreatment (Supplementary Data 3).

Following pretreatment, chemistry samples for radiocarbon dating were combusted using a PDZ-Europa Robo-Prep biological sample converter (combustion elemental analyzer) coupled to a PDZ-Europa 20/20 mass spectrometer operating in continuous flow mode using a Helium carrier gas. This enables $\delta^{15}\text{N}$ and $\delta^{13}\text{C}$, nitrogen and carbon

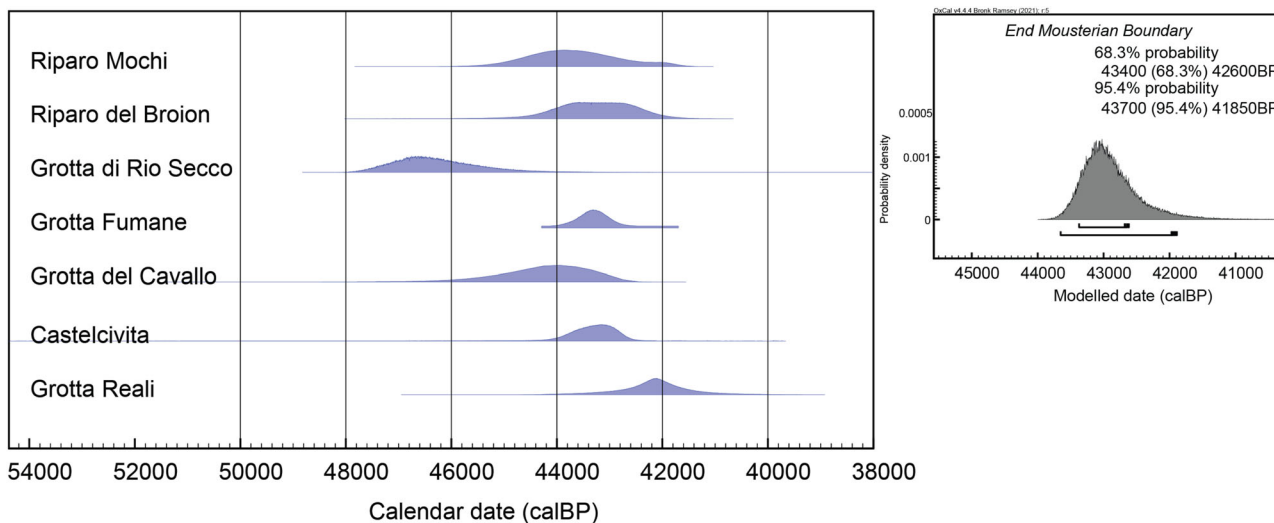


Fig. 8 | HPDs for end boundaries of the Mousterian at the sites studied (end boundaries from Riparo Mochi, Grotta di Fumane, Grotta di Rio Secco and Riparo Broion are included for comparison). Note that for Grotta Reali the Bayesian model of Peretto et al. (2020) does not contain any post-Mousterian constraint and has a

wide range, so we use the Reali Date HPD from the final Mousterian level instead, and this is included in this model (Supplementary Information). The inset shows the final Mousterian boundary calculated (see text for details).

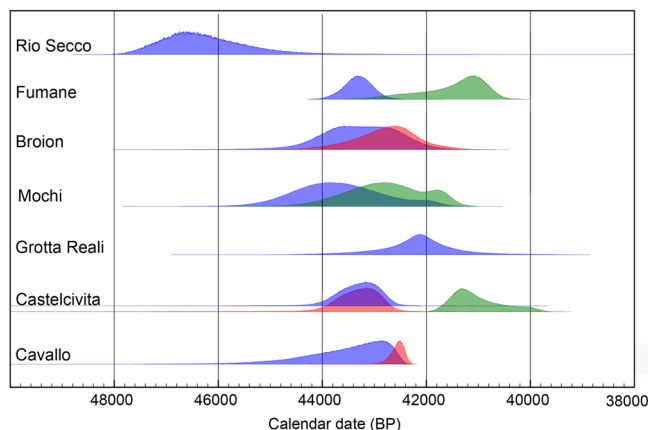


Fig. 9 | HPDs for the end boundaries of the Mousterian (blue), the start boundaries of the Uluzzian (red) and the start boundaries of the Protoaurignacian (green). Sites are plotted in order from north to south. Note that the Castelcivita Uluzzian start boundary is essentially the same distribution as for the end of the Mousterian, which is why the two HPDs are very slightly offset from one another in the figure. Fumane data is from Higham et al. (2011), and Mochi data comes from Frouin et al. (2022). The Rio Secco data is after Talamo et al. (2014), Grotta Reali after Peretto et al. (2020) and Broion from Romandini et al. (2012).

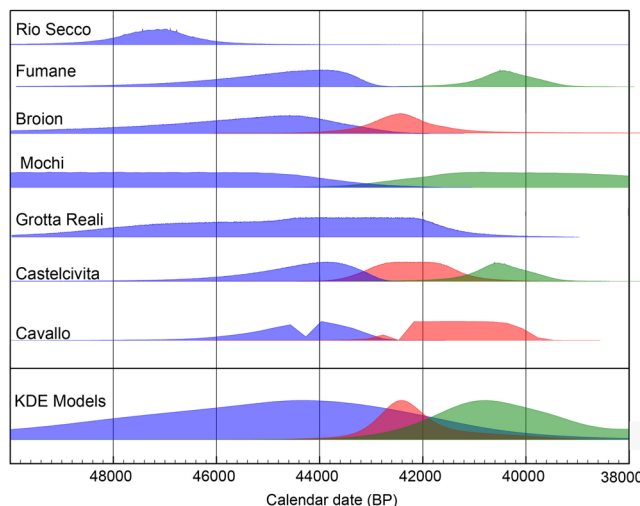


Fig. 10 | Date ranges for the key sites in Italy, below are the stacked KDE_Models we built for comparison on an Italian-wide scale. Once more, the Mousterian is blue, the Uluzzian red and the Protoaurignacian green. In the KDE_Model at the bottom, the green distribution includes both Proto- and Early Aurignacian determinations.

content, as well as C: N atomic ratios to be measured. We used VPDB as the standard for the $\delta^{13}\text{C}$ measurements and AIR for the $\delta^{15}\text{N}$ values. Graphite was produced by reacting the sample CO₂ over an iron catalyst in an excess H₂ atmosphere at 560 °C. AMS radiocarbon measurement was carried out using the ORAU 2.5MV HVEE accelerator and, after 2020, using an IonPlus MiCaDaS. In Supplementary Data 2–5, we report the data for failed samples and analytical data from the radiocarbon work.

Optically stimulated luminescence dating

Sampling and preparation. All samples for luminescence dating were selected on-site under controlled conditions (Supplementary Note 3). The samples and their contexts are given in Table 6.

Laboratory sample preparation involved the extraction of coarse quartz grains (180–255 μm) through wet sieving, hydrochloric acid (10%), and then hydrogen peroxide (30% for 72 h) digestions, heavy liquid density separations (sodium polytungstate solutions at 2.70 g cm⁻³ and 2.62 g cm⁻³), etching with hydrofluoric acid (40%) for 60 min, and finally washing with concentrated hydrochloric acid. The purified quartz-rich fraction was sieved and mounted on stainless steel cups using silicon oil as aliquots of ~4 mm diameter (for Castelcivita and Oscursciuto samples) or ~2 mm (for Cala samples).

Optical measurements were conducted on an automated *Lexsyg* research device at the LDL Research Laboratory for Archaeology and the History of Art (RLAHA) at the University of Oxford and further completed on a standard OSL/TL Risø device at the Luminescence Dating Research Laboratory at Stony Brook University. The *Lexsyg*

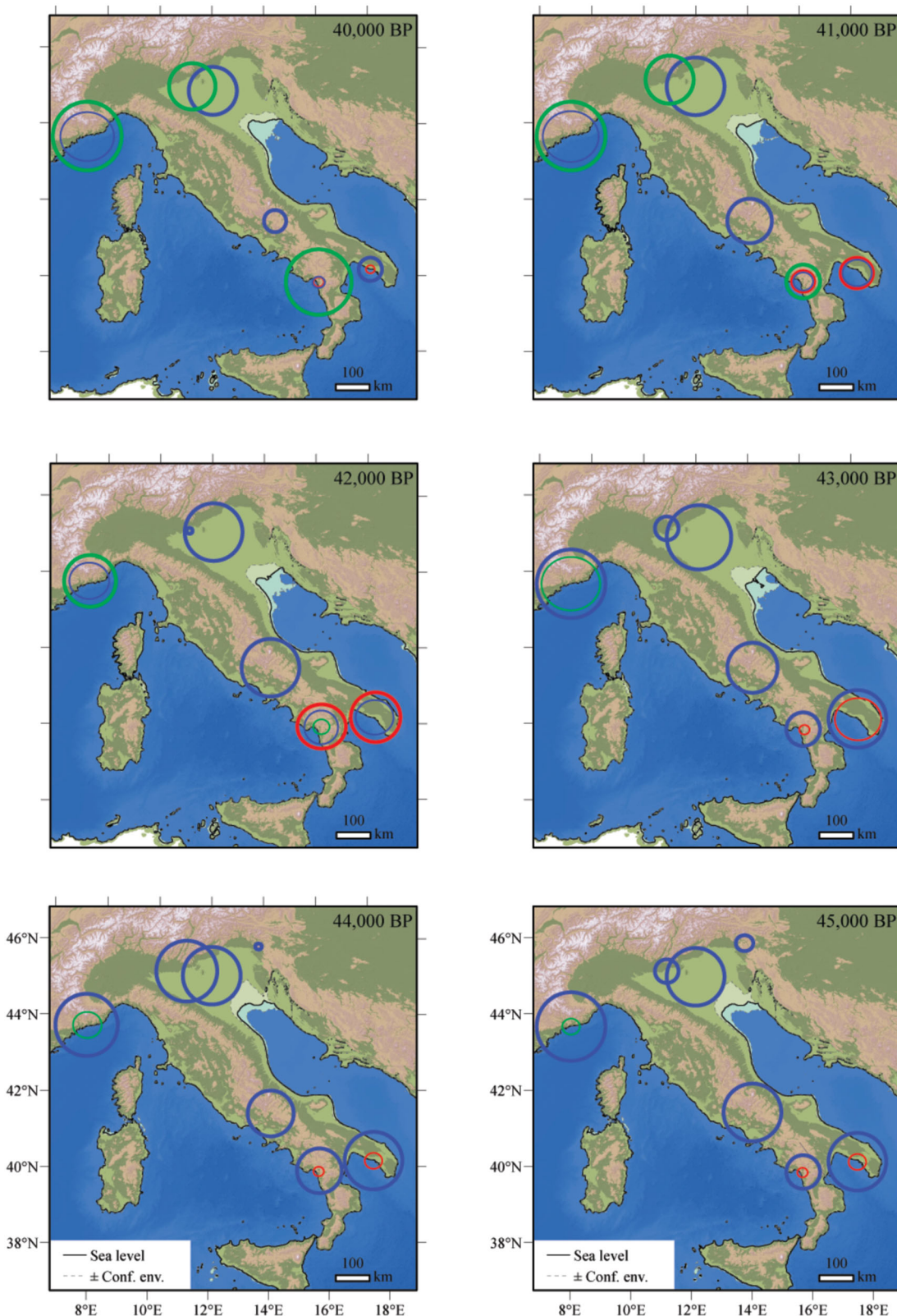


Fig. 11 | Spatio-temporal mapping of the Mousterian→Uluzzian→Aurignacian time spans in the Italian Peninsula, in the interval 45,000–40,000 BP. The data was generated using OxCal's `KDE_Model` approach. The circles indicate the variations of the KDE values at the selected time slice. Blue circles are the Mousterian, green circles are the Aurignacian and red are the Uluzzian. Note that for Riparo Broion, we

did not include the Uluzzian because there is only one determination, which is not sufficient for KDE modelling. The paleogeographic maps were generated using ArcGIS®10.8. Source of the Digital Elevation Model: EU-DEM. Source of the Bathymetry: EMODNET.

research device was equipped with a $^{90}\text{Sr}/^{90}\text{Y}$ ring-shaped irradiation source delivering ca. $0.068 \pm 0.001 \text{ Gy s}^{-1}$ at the sample position (calibrated using Risø calibration quartz batch 98 and corrected using the factor from ref. 92). The quartz was stimulated with blue LEDs emitting at $470 \pm 30 \text{ nm}$ covered by a long pass filter (3 mm Schott GG420). The resulting optically stimulated luminescence (OSL) signal was detected by a PMT (Hamamatsu H7360-02) through an optical filter (7.7 mm Hoya U-340; transmission between 290–370 nm). The absence of feldspars was checked for all the samples with a near-infra-red stimulation using LEDs emitting at $850 \pm 30 \text{ nm}$, and the luminescence signal was detected through a combination of 3 mm of Schott BG39 and 3.5 mm of AHF BrightLine HC 414/46 nm, giving a detection window centred on 410 nm.

Additional measurements were performed on an OSL/TL Risø-DA-20 equipped with a $^{90}\text{Sr}/^{90}\text{Y}$ source delivering ca. $0.106 \pm 0.003 \text{ Gy s}^{-1}$ (calibrated using Risø calibration quartz batch 123 and corrected using the factor from ref. 92) to the material deposited in the discs. The quartz OSL signal was stimulated with blue LEDs emitting at $470 \pm 20 \text{ nm}$. The resulting luminescence signals were collected by an EMI 9235 QA photomultiplier tube through a combination of optical filters (Schott BG3/Schott BG39). All measurements were performed in a nitrogen atmosphere.

Dosimetry. The doses of radiation to which the grains have been submitted during their burial originate from the decay of natural radioelements (mainly from the U and Th-series and from K) emitting ionising particles (alpha, beta, and gamma) in the surrounding sediments and by cosmic rays.

As the quartz grains were etched, no alpha dose contribution was considered. The beta dose rates were calculated from the K, U, and Th contents measured on a portion of sediment by ICP/MS and ICP/AES, considering the conversion factors of Guérin et al.⁹³ and the grain size attenuation factors of ref. 94. In Supplementary Note 3, we discuss the different approaches to dose rate calculation by site. The total dose rates (Supplementary Data 6) were calculated using the Dose Rate Calculator v1.2 developed by Durcan et al.⁹⁵

Paleogeographic reconstruction

For an improved contextualisation of the appearance/diffusion process of the Protoaurignacian and Uluzzian technocomplexes (and their relation with the Mousterian), we built a spatio-temporal series with paleogeographic maps for each 1000-year time-slice, from 45,000 to 40,000 BP. We used the OxCal4.3.3 model results and ArcGIS[®] 10.8, merging the EuroDEM (European Digital Elevation Model) and the EMODNET (European Marine Observation and Data Network) of the Mediterranean. The relative sea-levels (RSL) with the confidence intervals for each time slice have been derived from ref. 96. A raster calculator function has been adopted to modify the pixel values of the digital elevation models, according to the expected RSL of each time slice (e.g., ref. 97).

Reporting summary

Further information on research design is available in the Nature Portfolio Reporting Summary linked to this article.

Data availability

Supplementary data are contained in the linked Supplementary Information. This includes additional data concerned with the archaeological sites we studied, additional methods statements on ZooMS (Supplementary Note 5), radiocarbon dating and OSL, dose rate calculations (Supplementary Note 3) and Bayesian modelling (Supplementary Note 4).

Code availability

All OxCal CQL codes are included in the Supplementary Code 1 file.

References

- Hublin, J. J. The modern human colonization of western Eurasia: when and where? *Quat. Sci. Rev.* **118**, 194–210 (2015).
- Benazzi, S. et al. The makers of the Protoaurignacian and implications for Neandertal extinction. *Science* **348**, 793–796 (2015).
- Picin A., Moroni A., Benazzi S. The arrival of *Homo sapiens* in the Near East and Europe. In: Romagnoli F., Rivals F., Benazzi S. (eds.) *Updating Neanderthals. Understanding Behavioural Complexity in the Late Middle Palaeolithic*, Elsevier Academic Press, 321–336, (2022).
- Teyssandier, N. Us and them: how to reconcile archaeological and biological data at the middle-to-upper Palaeolithic transition in Europe? *J. Paleolit. Archaeol.* **7** (2024).
- Higham, T. F. G. et al. Problems with radiocarbon dating the middle to upper Palaeolithic transition in Italy. *Quat. Sci. Rev.* **28**, 1257–1267 (2009b).
- Higham, T. European Middle and Upper Palaeolithic radiocarbon dates are often older than they look: problems with previous dates and some remedies. *Antiquity* **85**, 235–249 (2011).
- Marciani, G. et al. Lithic techno-complexes in Italy from 50 to 39 thousand years BP: an overview of lithic technological changes across the middle-upper Palaeolithic boundary. *Quat. Int.* **551**, 123–149 (2020a).
- Carmignani, L. & Soressi, M. Ahead of the times: blade and bladelet production associated with Neandertal remains at the Bau de l'Aubesier (Mediterranean France) between MIS 7 and MIS 5d. *Paleo Anthropol.* **1**, 1–33 (2023).
- Bon, F. Little big tool. Enquête autour du succès de la lamelle. In: F. Le Brun-Ricalens (ed.) *Productions lamellaires attribuées à l'Aurignacien*, 479–484. MNHA, Luxembourg. (2005)
- Le Brun-Ricalens, F., Bordes, J.-G., Eizenberg, L. A crossed-glance between southern European and Middle-Near Eastern early Upper Palaeolithic lithic technocomplexes. Existing models, new perspectives. In: Camps, M., Szmidt, C. (Eds.) *The Mediterranean from 50 000 to 25 000 BP: Turning Points and New Directions*. Oxbow Books, Oxford, 11–33 (2009)
- Falcucci, A. et al. What's the point? Retouched bladelet variability in the Protoaurignacian. Results from Fumane, Isturitz, and Les Cottés. *Archaeol. Anthropol. Sci.* **10**, 539–554 (2018).
- Negrino F. and Riel-Salvatore J. From Neanderthals to anatomically modern humans in Liguria (Italy): the current state of knowledge. In: V. Borgia & E. Cristiani (eds.): *Palaeolithic Italy. Advanced studies on early human adaptations in the Apennine peninsula*, 161–181. Side-stone Press, Leiden. (2018).
- Broglia A. & Dalmeri G. Pitture paleolitiche nelle Prealpi Venete: Grotta di Fumane e Riparo Dalmeri. Memorie del Museo Civico di Storia Naturale di Verona, 2a serie, Sezione Scienze dell'Uomo, 9. Verona. (2005).
- Palma di Cesnola, A. Seconda campagna di scavi nella Grotta del Cavallo presso Santa Caterina (Lecce). *Riv. Sci. Preistoriche* **19**, 23–39 (1964).
- Benazzi, S. et al. Early dispersal of modern humans in Europe and implications for Neanderthal behaviour. *Nature* **479**, 525–528 (2011).
- Hublin, J. J. et al. Initial upper Palaeolithic homo sapiens from Bacho Kiro cave, Bulgaria. *Nature* **581**, 299–302 (2020).
- Slimak, L. et al. Modern human incursion into Neanderthal territories 54,000 years ago at Mandrin, France. *Sci. Adv.* **8**, eabj9496 (2022).
- Arrighi, S. et al. Bone tools, ornaments and other unusual objects during the middle to upper Palaeolithic transition in Italy. *Quat. Int.* **551**, 169–187 (2020a).
- Arrighi, S. et al. Backdating systematic shell ornament making in Europe to 45,000 years ago. *Archaeol. Anthropol. Sci.* **12**, 59 (2020b).

20. Arrighi, S. et al. Between the hammerstone and the anvil: bipolar knapping and other percussive activities in the late Mousterian and the Uluzzian of Grotta di Castelcivita (Italy). *Archaeol. Anthropol. Sci.* **12**, 271 (2020c).
21. Boscato, P. & Crezzini, J. Middle-Upper Palaeolithic transition in Southern Italy: Uluzzian macromammals from Grotta del Cavallo (Apulia). *Quat. Int.* **252**, 90–98 (2012).
22. Collina, C. et al. Refining the Uluzzian through a new lithic assemblage from Roccia San Sebastiano (Mondragone, southern Italy). *Quat. Int.* **551**, 150–168 (2020).
23. Crezzini, J., Boscato, P., Ronchitelli, A. & Boschin, F. A peculiar exploitation of ungulates at Grotta di Santa Croce: bone grease rendering and nutritional patterns among Neanderthals in southern Italy. *Hist. Biol.* <https://doi.org/10.1080/08912963.2023.2242630>. (2023).
24. Moroni, A. et al. Grotta del Cavallo (Apulia—Southern Italy). The Uluzzian in the mirror. *J. Anthropol. Sci.* **96**, 125–160 (2018).
25. Rossini, M. et al. Less is more! Uluzzian technical behaviour at the cave site of Castelcivita (southern Italy). *J. Archaeol. Sci. Rep.* **44**, 103494 (2022).
26. Sano, K. et al. The earliest evidence for mechanically delivered projectile weapons in Europe. *Nat. Ecol. Evol.* **3**, 1409–1414 (2019).
27. Zilhão, J., Banks, W. E., d'Errico, F. & Gioia, P. Analysis of site formation and assemblage integrity does not support attribution of the Uluzzian to modern humans at Grotta del Cavallo. *PLoS One* **10**, e0131181 (2015).
28. Mylopotamitaki, D. et al. Homo sapiens reached the higher latitudes of Europe by 45,000 years ago. *Nature* **626**, 341–346 (2024).
29. Demidenko, Y. E. & Škrdla, P. Lincombian-Ranisian-Jerzmanowician industry and South Moravian sites: a Homo sapiens late initial upper Paleolithic with Bohunician industrial generic roots in Europe. *J. Paleolit. Archaeol.* **6**, 17 (2023).
30. Djakovic, I., Roussel, M., Soressi, M. Prospects and pitfalls of an intrusive model for the Châtelperronian stone tool industry during the Middle to Upper Palaeolithic transition in France and northern Spain. Preprint. <https://doi.org/10.1101/2023.07.14.549013>, (2023).
31. Gicqueau, A. et al. Anatomically modern human in the Châtelperronian hominin collection from the Grotte du Renne (Arcy-sur-Cure, Northeast France). *Sci. Rep.* **13**, 12682 (2023).
32. Peresani, M., Bertola, S., Delpiano, D., Benazzi, S. & Romandini, M. The Uluzzian in the north of Italy: insights around the new evidence at Riparo Broion. *Archaeol. Anthropol. Sci.*, **11**, 3503–3536 (2019).
33. Dini, M. & Tozzi, M. La transizione Paleopolitico medio-Paleopolitico superiore nella Grotta La Fabbrica (Grosseto -Toscana). *Atti. Soc. Toscana Sci. Nat. Pisa, P. V. Mem. Ser. B* **117–119**, 17–25 (2012).
34. Villa, P. et al. From Neandertals to modern humans: new data on the Uluzzian. *PLoS One* **13**, e0196786 (2018).
35. Palma di Cesnola, A. Il Paleopolitico della Puglia (giacimenti, periodi, problemi). *Mem. del. Mus. Civ. di Stor. Nat. Verona* **7**, 1–84 (1967).
36. Zanchetta, G., Giaccio, B., Bini, M. & Sarti, L. Tephrostratigraphy of Grotta del Cavallo, Southern Italy: insights on the chronology of middle to upper Palaeolithic transition in the Mediterranean. *Quat. Sci. Rev.* **182**, 65–77 (2018).
37. Giaccio, B., Hajdas, I., Isaia, R., Deino, A. & Nomades, S. High-precision ^{14}C and $^{40}\text{Ar}/^{39}\text{Ar}$ dating of the Campanian Ignimbrite (Y-5) reconciles the time-scales of climatic-cultural processes at 40ka. *Sci. Rep.* **7**, 45940 (2017).
38. Fabbri, P. F., Vincenti, G. I fossili umani neandertaliani. In: Sarti, L., Martini, F. (ed.) *Il Musteriano di Grotta del Cavallo nel Salento (scavi 1986-2005). Culture e ambienti*. Millenni, 23, Firenze, 515–527 (2020).
39. Wood, R. E. et al. Testing the ABOx-SC method: dating known-age charcoals associated with the Campanian Ignimbrite. *Quat. Geochronol.* **9**, 16–26 (2012).
40. Douka, K. et al. On the chronology of the Uluzzian. *J. Hum. Evol.* **68**, 1–13 (2014).
41. Martini, I. et al. Cave clastic sediments as a tool for refining the study of human occupation of prehistoric sites: insights from the cave site of La Cala (Cilento, southern Italy). *J. Quat. Sci.* **33**, 586–596 (2018).
42. Azzi, C. M., Bigliocca, L., Gulisano, F. Florence radiocarbon dates III. *Radiocarbon* **19**, 165–169 (1977).
43. Benini, A., Boscato, P. & Gambassini, P. Grotta della Cala (Salerno): Industrie Litiche e Faune Uluzziane ed Aurignaziane. *Riv. Sci. Preist.* **48**, 37–96 (1997).
44. Spagnolo, V. et al. Between hearths and volcanic ash: the SU 13 palimpsest of the Oscurusciuto rock shelter (Ginosa—Southern Italy): analytical and interpretative questions. *Quat. Int.* **417**, 105–121 (2016).
45. Spagnolo, V. et al. Neanderthal activity and resting areas from stratigraphic unit 13 at the middle Palaeolithic site of Oscurusciuto (Ginosa—Taranto, Southern Italy). *Quat. Sci. Rev.* **217**, 169–193 (2019).
46. Spagnolo, V. et al. Climbing the time to see Neanderthal behaviour's continuity and discontinuity: SU 11 of the Oscurusciuto Rockshelter (Ginosa, Southern Italy). *Archaeol. Anthropol. Sci.* **12**, 54 (2020).
47. Marciani, G. et al. Neanderthal occupation during the tephra fallout: Technical and hunting behaviours, sedimentology and settlement patterns in SU 14 of Oscurusciuto rock shelter (Ginosa, southern Italy). *Archaeol. Anthropol. Sci.* **12**, 152 (2020b).
48. Martini, I., Baucon, A. & Boschin, F. Depositional processes and environmental settings in rock shelters: the case of the prehistoric Oscurusciuto site (Southern Italy). *Geol. Mag.* **158**, 891–904 (2021).
49. Boscato, P. and Ronchitelli, A. Strutture di combustione in depositi del Paleopolitico medio del Sud Italia. *Int. J. Anthropol. (numero speciale)*, 218–225 (2008).
50. Devèse, T., Comeskey, D., McCullagh, J., Bronk Ramsey, C. & Higham, T. New protocol for compound-specific radiocarbon analysis of archaeological bones. *Rapid Commun. Mass Spectrom.* **32**, 373–379 (2018).
51. Bronk Ramsey, C. Bayesian analysis of radiocarbon dates. *Radiocarbon* **51**, 337–360 (2009).
52. Reimer, P. J. et al. The IntCal20 northern hemisphere radiocarbon age calibration curve (0–55 cal kBP). *Radiocarbon* **62**, 725–757 (2020).
53. Heaton, T. J. et al. Marine20—the marine radiocarbon age calibration curve (0–55,000 cal BP). *Radiocarbon* **62**, 779–820 (2020).
54. Svensson, A. et al. A 60,000-year Greenland stratigraphic ice core chronology. *Climate* **4**, 47–58 (2008).
55. Douka, K. Investigating the chronology of the Middle to Upper Palaeolithic transition in Mediterranean Europe by improved radiocarbon dating of shell ornaments. Unpublished D. Phil. in Archaeological Science, (University of Oxford, U.K., 2011).
56. McCarty, M. ZooMS analysis and radiocarbon dating of Grotta del Cavallo (Apulia, Italy) and implications on middle-to-upper paleolithic environmental changes and hominin behavior. Unpublished Master Dissertation, University of Oxford. (2021).
57. Reimer, P. J. & Reimer, R. W. A marine reservoir correction database and on-line interface. *Radiocarbon* **43**, 461–463 (2001).
58. Fabbri, P. F. et al. Middle Paleolithic human deciduous incisor from Grotta del Cavallo, Italy. *Am. J. Phys. Anthropol.* **161**, 506–512 (2016).
59. Frouin, M. et al. A refined chronology for the Middle and early Upper Paleolithic sequence of Riparo Mochi (Liguria, Italy). *J. Hum. Evol.* **169**, 103211 (2022).
60. Higham, T. et al. The timing and spatiotemporal patterning of Neanderthal disappearance. *Nature* **512**, 306–309 (2014).
61. Talamo, S. et al. Detecting human presence at the border of the northeastern Italian Pre-Alps. ^{14}C dating at Rio Secco Cave as

- expression of the first Gravettian and the late Mousterian in the northern Adriatic region. *PLoS One* **9**, e95376 (2014).
62. Romandini, M. et al. A late Neanderthal tooth from northeastern Italy. *J. Hum. Evol.* **147**, 102867 (2020).
 63. Peretto, C. et al. Grotta Reali, the first multilayered moustierian evidences (sic) in the Upper Volturno Basin (Rocchetta a Volturno, Molise, Italy). *Archaeol. Anthropol. Sci.* **12**, 67 (2020).
 64. Oxilia, G. et al. Direct evidence that late Neanderthal occupation precedes a technological shift in southwestern Italy. *Am. J. Biol. Anthropol.* **179**, 18–30 (2022).
 65. Peresani, M., Cristiani, E. & Romandini, M. The Uluzzian technology of Grotta di Fumane and its implication for reconstructing cultural dynamics in the middle–upper Palaeolithic transition of Western Eurasia. *J. Hum. Evol.* **91**, 36–56 (2016).
 66. Bronk Ramsey, C. Methods of summarizing radiocarbon datasets. *Radiocarbon* **59**, 1809–1833 (2017).
 67. Gambassini, P. Il Paleolitico di Castelcivita: Culture e Ambiente. *Electa, Napoli*, 160 pp (1997).
 68. Moroni, A., Boscato, P. & Ronchitelli, A. What roots for the Uluzzian? Modern behaviour in Central-Southern Italy and hypotheses on AMH dispersal routes. *Quat. Int.* **316**, 27–44 (2013).
 69. Moroni, A., Boscato, P. & Ronchitelli, A. The origin of the Uluzzian: the upsetting of a paradigm?. *Bull. Mus. Anthropol. préhist. Monaco* **56**, 136–139 (2016).
 70. Palma di Cesnola, A. Il Paleolitico superiore in Italia. *Garlatti e Razzai, Firenze* (1993).
 71. Spennato, A. G. I livelli protoaurignaziani della Grotta di Serra Cicora (Nardò—Lecce). *Stud. Eco. Quat.* **3**, 61–76 (1981).
 72. Fu, Q. et al. The genome sequence of a 45,000-year-old modern human from western Siberia. *Nature* **514**, 445–449 (2014).
 73. Fu, Q. et al. An early modern human from Romania with a recent Neanderthal ancestor. *Nature* **524**, 216–219 (2015).
 74. Hajdinjak, M. et al. Initial upper Palaeolithic humans in Europe had recent Neanderthal ancestry. *Nature* **592**, 253–257 (2021).
 75. Prüfer, K. et al. A genome sequence from a modern human skull over 45,000 years old from Zlatý kůň in Czechia. *Nat. Ecol. Evol.* **5**, 820–825 (2021).
 76. Vallini, L. et al. Genetics and material culture support repeated expansions into paleolithic eurasia from a population hub out of Africa. *Genome Biol. Evol.* **14**, evac045 (2022).
 77. Marsh, E. J., Korpisaari, A., Mundt, S. P., Gasco, A. & Durán, V. Radiocarbon vs. luminescence dating of archaeological ceramics in the southern Andes: a review of paired dates, bayesian models, and a pilot study. *Radiocarbon* **63**, 1471–1501 (2021).
 78. Reimer, P. J. Composition and consequences of the IntCal20 radiocarbon calibration curve. *Quat. Res.* **96**, 22–27 (2020).
 79. Muscheler, R. et al. Testing and improving the IntCal20 calibration curve with independent records. *Radiocarbon* **62**, 1079–1094 (2020).
 80. Brock, F. & Higham, T. F. G. AMS radiocarbon dating of Paleolithic-aged charcoal from Europe and the Mediterranean Rim using ABOx-SC. *Radiocarbon* **51**, 839–846 (2009).
 81. Bird, M. I. et al. Radiocarbon dating of “old” charcoal using a wet oxidation, stepped-combustion procedure. *Radiocarbon* **41**, 127–140 (1999).
 82. Douka, K. et al., in prep. Radiocarbon dating of charcoal using a modified ABOx-SC approach. In: *Japan Geoscience Union Meeting* (2004).
 83. Bird, M. I. et al. Radiocarbon dating from 40 to 60 ka BP at Border Cave, South Africa. *Quat. Sci. Rev.* **22**, 943–947 (2003).
 84. Douka, K., Higham, T. & Sinitsyn, A. The influence of pretreatment chemistry on the radiocarbon dating of Campanian Ignimbrite-aged charcoal from Kostenki 14 (Russia). *Quat. Res.* **73**, 583–587 (2010).
 85. Higham, T. F. G. et al. Radiocarbon dating of charcoal from tropical sequences: results from the Niah Great Cave, Sarawak and their broader implications. *J. Quat. Sci.* **24**, 189–197 (2009).
 86. Santos, G. M. et al. A revised chronology of the lowest occupation layer of Pedra Furada Rock Shelter, Piauí, Brazil: the Pleistocene peopling of the Americas. *Quat. Sci. Rev.* **22**, 2303–2310 (2003).
 87. Turney, C. S. et al. Early human occupation at Devil’s Lair, southwestern Australia 50,000 years ago. *Quat. Res.* **55**, 3–13 (2001).
 88. Zhang, J. F. et al. Radiocarbon and luminescence dating of the Wulanmulun site in Ordos, and its implication for the chronology of Paleolithic sites in China. *Quat. Geochronol.* **72**, 101371 (2022).
 89. Brock, F., Higham, T., Ditchfield, P. & Bronk Ramsey, C. Current pretreatment methods for AMS radiocarbon dating at the Oxford Radiocarbon Accelerator Unit (Orau). *Radiocarbon* **52**, 103–112 (2010).
 90. Brock, F., Ramsey, C. B. & Higham, T. Quality assurance of ultra-filtered bone dating. *Radiocarbon* **49**, 187–192 (2007).
 91. Falucci, A. et al. Pre-Campanian Ignimbrite techno-cultural shift in the Aurignacian sequence of Grotta di Castelcivita, southern Italy. *Sci. Rep.* **14**, 12783 (2024).
 92. Autzen, M., Andersen, C. E., Bailey, M. & Murray, A. S. Calibration quartz: an update on dose calculations for luminescence dating. *Radiat. Meas.* **157**, 106828 (2022).
 93. Guérin, G., Mercier, N. & Adamiec, G. Dose-rate conversion factors: update. *Anc. Tl* **29**, 5–8 (2011).
 94. Guérin, G., Mercier, N., Nathan, R., Adamiec, G. & Lefrais, Y. On the use of the infinite matrix assumption and associated concepts: a critical review. *Radiat. Meas.* **47**, 778–785 (2012).
 95. Durcan, J. A., King, G. E. & Duller, G. A. T. DRAC: dose rate and age calculator for trapped charge dating. *Quat. Geochronol.* **28**, 54–61 (2015).
 96. Waelbroeck, C. et al. Sea-level and deep water temperature changes derived from benthic foraminifera isotopic records. *Quat. Sci. Rev.* **21**, 295–305 (2002).
 97. Conti, E. et al. Back to the Past. The paleogeography as key to understand the Middle Palaeolithic peopling at Grotta dei Santi (Mt Argentario—Tuscany). *Acta IMEKO* **12**, 35 (2023).
 98. Tassoni, L. Gli ornamenti su conchiglia dell’Uluzziano e del Proto-Aurignaziano delle Grotte di Castelcivita e della Cala (SA): studio tassonomico, tafonomico e sperimentale. Unpublished Master Dissertation, University of Ferrara (2018–2019).

Acknowledgements

We are grateful to the European Research Council (ERC) for funding. The European Union’s Seventh Framework Programme (FP7/2007–2013) ERC grant 324139 “PalaeoChron” awarded to TH, funded the chronometric work, and the European Union’s Horizon 2020 research and innovation programme (ERC grant 724046—SUCCESS), awarded to S.B., funded research at Cala and Castelcivita. We are also grateful to the PRIN 2022 TRACE project which awarded funding to S.B. and A.M. Research at the sites studied has received funding from the University of Siena, the Centro Studi sul Quaternario, the National Geographic Society (Exploration Grant Programme, grant NGS-61617R-19), the Municipalities of Camerota and Ginosa and the Società Grotte di Castelcivita. We thank all members of the project, as well as our friends and colleagues at the Oxford Radiocarbon Accelerator Unit and Research Laboratory for Archaeology and the History of Art, University of Oxford for their input. We are deeply grateful to Professors Palma di Cesnola and Paolo Gambassini for their professionalism, dedication, and the great sense of responsibility with which they conducted research at the caves of Cavallo, Cala and Castelcivita, thereby providing us today with the opportunity to study the materials from their excavations. Finally, we thank the reviewers for their excellent and constructive suggestions and comments on this paper. Open access funding provided by University of Vienna.

Author contributions

The project was conceived by all authors. Radiocarbon dating was undertaken by T.H., K.D., M.M. and T.D. O.S.L. dating was done by M.F. and J.L.S. Bayesian modelling was undertaken by T.H. Archaeological

fieldwork/materials were undertaken by A.R., P.B., S.B., J.C., V.S., G.M., A.F., M.R., S.A., C.D., I.M., A.M. and F.B. The original draft was written by T.H., A.M. and F.B., and all authors contributed, reviewed and edited. Figure 1 was made by S.A, Figs. 2 and 11, S1–4 were made by V.S., T.H. produced Figs. 3–10. Paleogeographic reconstructions were done by V.S. Scientific direction of the research project at Castelcivita and Cala: A.M. and A.R. Scientific direction of the research project at Oscrusciuto: F.B., A.R. and P.B. Scientific direction of the research project on the Uluzzian of Cavallo: A.M.

Competing interests

The authors declare no competing interests.

Additional information

Supplementary information The online version contains supplementary material available at <https://doi.org/10.1038/s41467-024-51546-9>.

Correspondence and requests for materials should be addressed to Tom Higham, Marine Frouin or Francesco Boschin.

Peer review information *Nature Communications* thanks Erik Marsh and the other, anonymous, reviewer(s) for their contribution to the peer review of this work. A peer review file is available.

Reprints and permissions information is available at <http://www.nature.com/reprints>

Publisher's note Springer Nature remains neutral with regard to jurisdictional claims in published maps and institutional affiliations.

Open Access This article is licensed under a Creative Commons Attribution-NonCommercial-NoDerivatives 4.0 International License, which permits any non-commercial use, sharing, distribution and reproduction in any medium or format, as long as you give appropriate credit to the original author(s) and the source, provide a link to the Creative Commons licence, and indicate if you modified the licensed material. You do not have permission under this licence to share adapted material derived from this article or parts of it. The images or other third party material in this article are included in the article's Creative Commons licence, unless indicated otherwise in a credit line to the material. If material is not included in the article's Creative Commons licence and your intended use is not permitted by statutory regulation or exceeds the permitted use, you will need to obtain permission directly from the copyright holder. To view a copy of this licence, visit <http://creativecommons.org/licenses/by-nc-nd/4.0/>.

© The Author(s) 2024

¹Department of Evolutionary Anthropology, Faculty of Life Sciences, University Biology Building, University of Vienna, Djerassiplatz 1, A-1030 Vienna, Austria.

²Human Evolution and Archaeological Sciences (HEAS) Forschungsverbund, University of Vienna, Vienna, Austria. ³Department of Geosciences and Turkana Basin Institute, Stony Brook University, 255 Earth and Space Science Building, Stony Brook, Long Island, NY, USA. ⁴Dipartimento di Scienze Fisiche, della Terra e dell'Ambiente, Università degli Studi di Siena (UniSI), Strada Laterina, 8, 53100 Siena, Italy. ⁵Dipartimento di Beni Culturali, Università degli Studi di Bologna (UniBO), Via degli Ariani 1, 48121 Ravenna, Italy. ⁶Department of Biology, University of Florence, Via del Proconsolo 12, 50122 Florence, Italy. ⁷Centro Studi sul Quaternario ODV, Via Nuova dell'Ammazzatoio, 7, 52037 Sansepolcro, AR, Italy. ⁸School of Life Sciences, Arizona State University, Tempe, AZ, USA.

⁹Department of Geosciences, Prehistory and Archaeological Sciences Research Unit, Eberhard Karls University of Tübingen, Tübingen, Germany. ¹⁰CEREGE, Aix-Marseille University, CNRS, IRD, INRAE, Collège de France, Technopôle de l'Arbois, 13545 Aix-en-Provence, France. ¹¹Luminescence Laboratory, Research Laboratory for Archaeology and the History of Art, University of Oxford, Oxford OX13QY, United Kingdom. ¹²These authors contributed equally: Tom Higham, Marine Frouin, Adriana Moroni, Francesco Boschin.  e-mail: thomas.higham@univie.ac.at; marine.frouin@stonybrook.edu; francesco.boschin@unisi.it